MDPI

Review

Review of Emission Characteristics and Purification Methods of Volatile Organic Compounds (VOCs) in Cooking Oil Fume

Chong Tao [1], Limo He [1,*], Xuechen Zhou [1], Hanjian Li [1], Qiangqiang Ren [1], Hengda Han [1], Song Hu [1,2,*], Sheng Su [1,2], Yi Wang [1,2] and Jun Xiang [1,2]

[1] State Key Laboratory of Coal Combustion, School of Energy and Power Engineering, Huazhong University of Science and Technology, Wuhan 430074, China

[2] China-EU Institute for Clean and Renewable Energy, Huazhong University of Science and Technology, Wuhan 430074, China

* Correspondence: limo_615@163.com (L.H.); husong_hust@hotmail.com (S.H.)

Abstract: Volatile organic compounds (VOCs) in cooking oil fumes need to be efficiently removed due to the significant damage they cause to the environment and human health. This review discusses the emission characteristics, which are influenced by different cooking temperatures, cooking oils, and cuisines. Then, various cooking oil fume purification methods are mainly classified into physical capture, chemical decomposition, and combination methods. VOCs removal rate, system operability, secondary pollution, application area, and cost are compared. The catalytic combustion method was found to have the advantages of high VOC removal efficiency, environmental protection, and low cost. Therefore, the last part of this review focuses on the research progress of the catalytic combustion method and summarizes its mechanisms and catalysts. The Marse-van Krevelen (MVK), Langmuir-Hinshelwood (L-H), and Eley-Rideal (E-R) mechanisms are analyzed. Noble metal and non-noble metal catalysts are commonly used. The former showed excellent activity at low temperatures due to its strong adsorption and electron transfer abilities, but the high price limits its application. The transition metals primarily comprise the latter, including single metal and composite metal catalysts. Compared to single metal catalysts, the interaction between metals in composite metal catalysts can further enhance the catalytic performance.

Keywords: cooking oil fume; VOCs; emission characteristics; purification methods; catalytic combustion

1. Introduction

Cooking oil fumes have become the third largest source of urban air pollution, after pollutant gases from vehicles and industry. Besides, cooking oil fumes and smoking are considered the two major contributors to indoor pollution, leading to a remarkable increase in the cancer population, particularly among non-smoking women [1,2].

Cooking oil fumes are created by the oxidative decomposition of fats, lipids, and organic matter and their secondary reaction of the cracking of intermediate products at high temperatures. There are at least 300 components that contain a large amount of volatile organic compounds (VOCs), such as fatty acids, alkanes, alkenes, ketones, aldehydes, alcohol esters, aromatic, and heterocyclic compounds. They are hazardous to the environment and human health and difficult to remove with current purification equipment [3–10]. Many researchers found that the VOCs could react with NO_x and oxidants such as O_3 to form more serious pollutants such as photochemical smog and organic aerosols, respectively. Mauderly et al. [11] found that organic compounds affect the respiratory and cardiovascular systems and are difficult to remove. Billionnet et al. [12] described the hazards of air pollutants containing VOCs and showed that further research is needed on the factors affecting the pollutants. In addition, studies have shown that the ketones and aldehydes in cooking oil fumes have irritating effects on mucous membranes and the respiratory tract, which can

cause nausea, headaches, and other adverse reactions [13–18]. Although there is a small percentage of polycyclic aromatic hydrocarbons (PAHs), they have terrible carcinogenicity and are the leading cause of lung cancer [19]. Furthermore, the VOCs can cause different biological effects such as gene mutation and chromosomal damage, which are mutagenic and genotoxic [20]. Therefore, removing VOCs from cooking oil fumes is essential and urgent. There are various purification methods for cooking oil fumes, and the catalytic combustion method has great potential for application due to its characteristics of high efficiency and environmental protection. As a crucial part of this method, catalysts have been a hot research topic. Rao et al. and Zhang et al. summarized the research progress of metal-organic framework-based and derivative materials and zeolites in catalytic oxidation of VOCs, respectively [21,22]. These catalysts have great potential for application in the removal of cooking oil fumes. However, to better purify VOCs in cooking oil fume, the emission characteristics, the selection of purification methods, and the development of catalysts need to be further explored.

The components of VOCs are determined by the cooking foods, oils, and conditions, which consequently influence the toxic hazard and removal efficiency of the purification process. Thus, in this review, the emission characteristics of VOCs will be analyzed first. Then, updated purification methods, divided into physical capture, chemical decomposition, and combination methods, are compared in several aspects of removal rate, cost, and application area. Among them, the catalytic combustion method is the most effective way to convert the VOCs into CO_2 and H_2O at low temperatures, which has the advantages of high removal efficiency, low cost, and environmental friendliness. Finally, this review focuses on the analysis of the catalytic combustion process. The catalytic mechanism and the effects of different VOCs components and catalysts are compared and analyzed. Various types of catalysts have been used to date. This review divides them into two categories: noble metal catalysts and non-noble metal oxide catalysts. This review analyzes the emission characteristics, overall removal technologies, and catalytic combustion method for VOCs in cooking oil fume, all of which aid in the purification of indoor and outdoor pollution caused by cooking oil fumes.

2. Emission Characteristics of VOCs in Cooking Oil Fume

Cooking oil fume contains complex and diverse components, including hydrocarbons, ketone aldehydes, alcohol ethers, acid esters, polycyclic compounds, and other species. Their boiling points and production conditions affect the composition and concentration of cooking oil fume under various conditions, such as cooking oil, temperature, and types of cuisine [23–30].

2.1. Influence of Cooking Oils

Different oils have different constituents and chemical properties, resulting in differences in the components and concentrations of VOCs. Zhang et al. [31] took oils commonly used in Chinese cooking (rapeseed oil, soybean oil, peanut oil, corn oil, and lard oil) as examples to study the emission of VOCs. The results showed that the order of emission concentration was: rapeseed oil (81.0 mg/m^3) > soybean oil (75.5 mg/m^3) > peanut oil (70.9 mg/m^3) > corn oil (60.3 mg/m^3) > lard oil (20.5 mg/m^3). This is because cooking oils made from different raw materials have different contents and types of fatty acids, resulting in differences in their VOC emission characteristics [32,33]. In general, unsaturated fatty acids rich in double bonds (oleic acid, linolenic acid, linoleic acid, etc.) are more easily oxidized than saturated fatty acids, producing more aldehydes, alkanes, and olefins. This makes vegetable oils rich in unsaturated fatty acids, which release more VOCs than lard. He et al. [34] measured the concentration of five different cooking oil fumes at 260 °C and found that the emission concentrations of VOCs were in the following order: olive oil > peanut oil > sunflower oil > soybean oil > blend oil. As the distributions of the detected VOCs components shown in Figure 1 indicate, the distribution pattern is similar. Five different cooking oils produced the same major VOCs components at the same test

temperature of 260 °C and had similar concentration ratios between the components. The highest content was found in aldehydes, followed by hydrocarbons (olefin and alkane) and alcohols, with small amounts of furans and halohydrocarbons. In general, the concentration ranking of aldehydes, hydrocarbons, and alcohols with high content is basically the same. While there are differences in the concentration ranking of furans and halohydrocarbons with little content.
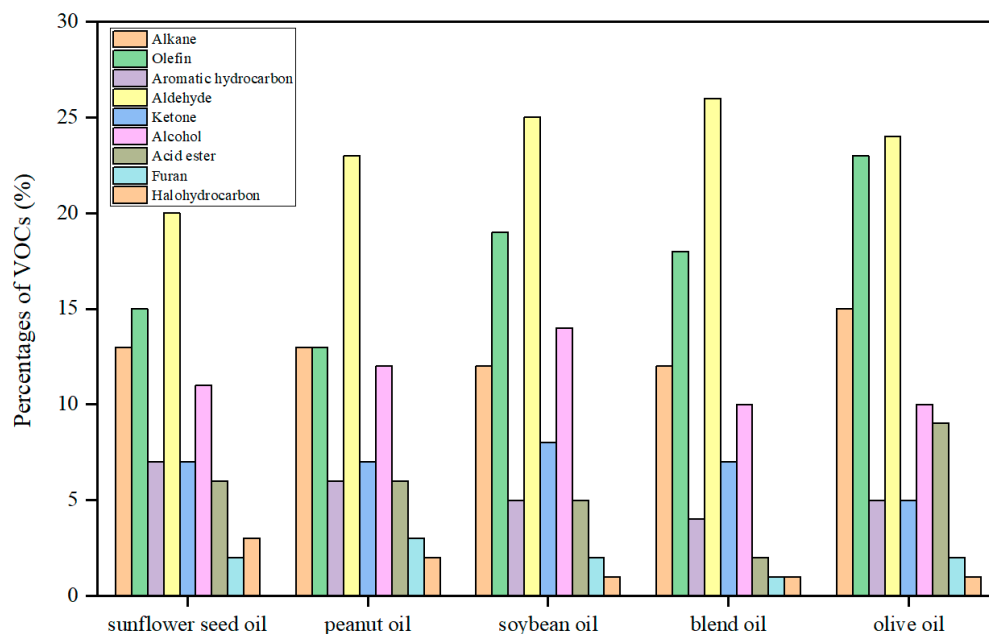

Figure 1. Distribution of VOCs in different cooking oils at 260 °C [34].

2.2. Influence of Cooking Temperatures

There is also research on the effect of temperature on VOC emissions, as temperature is an important factor affecting physicochemical reactions. Zhang and He et al. [31,34] studied the effect of temperature on the emission concentration of VOCs in soybean oil and sunflower oil, respectively. They found that the concentration and component of VOCs from both oils increased significantly with increasing temperature. For example, the mass concentration of VOCs in sunflower oil increased from 344.7 $\mu g/m^3$ to 2613.9 $\mu g/m^3$ when the temperature was increased from 130 to 260 °C, while the number of identifiable organic species increased from 41 to 86 species. Figure 2 shows the release of VOCs in sunflower oil between 130 and 260 °C. As shown in Figure 2, the VOCs components were mainly aldehydes, olefins, and alkanes, accounting for more than half of the total detected VOCs concentration, followed by alcohols, acid esters, ketones, and aromatic hydrocarbons, containing small amounts of furans and halogenated hydrocarbons. This is because heating significantly increases the decomposition rate of fatty acids and volatilizes more organic compounds with higher boiling points, which leads to an increase in both concentrations and components of VOCs [35]. Similar component distribution rules also apply to other oils, such as peanut oil and soybean oil. It can be seen that temperature is an extremely important factor in the emission of VOCs, and reasonable adjustment of cooking temperature plays a key role in controlling the generation of VOCs.
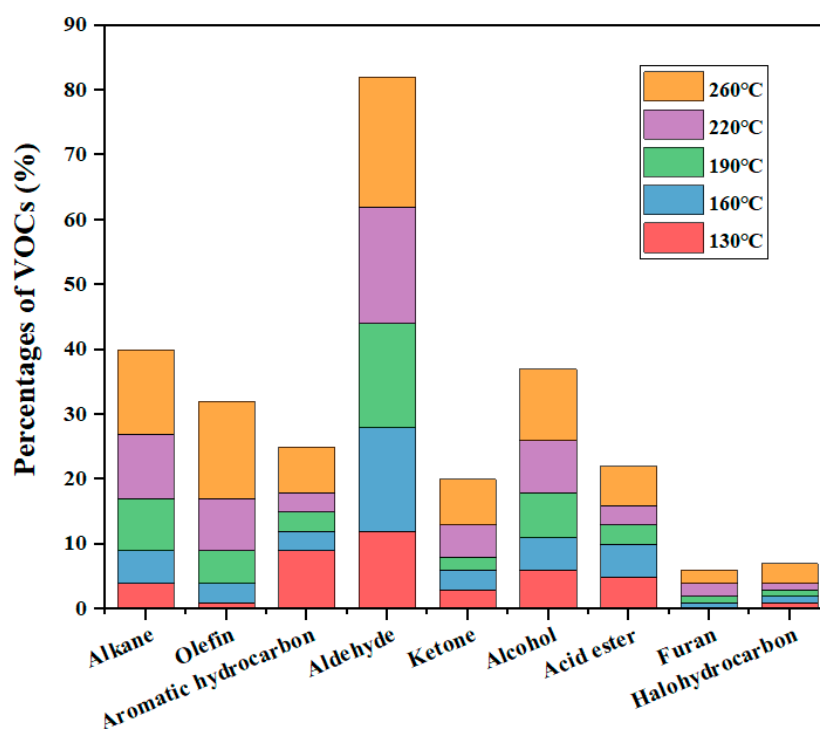
Figure 2. Distribution of VOCs in sunflower oil from 130 °C to 260 °C [34].

2.3. Influence of Cuisines

The cuisine type significantly affects the VOC emission concentration and composition. Compared to other countries, most studies on VOC emissions in different cuisines focus on Chinese cuisine due to the variety of cooking styles. As listed in Table 1, the emission rules are similar, although different measurement methods and standards may result in differences in the emission results from the same cuisine in various published literature [36–38]. The emission concentration of barbecue cuisine is significantly higher than that of non-grill cuisine, and there are also some differences in the emission concentration between non-grill dishes. Different cuisines greatly impact the emission of VOCs, especially barbecue cuisine, which should pay more attention to purification. Figure 3 shows the mass concentration percentage of VOCs in different cuisines. The result shows that the VOCs emitted by barbecue cuisine are mainly composed of hydrocarbon compounds. In non-grill cuisines, the content of alcohol increases, which, together with alkanes and aldehydes, constitutes the main pollutants. In addition to common domestic cuisines, different cooking styles at home and abroad can also lead to different emissions. In foreign countries, especially in some western countries, the cooking methods are relatively simple, and the food is mainly processed into semi-finished products, reducing the concentration of kitchen oil fumes. However, Chinese eating habits are quite different, and various cooking methods, such as frying, roasting, steaming, boiling, and stewing, result in a higher concentration of cooking oil fumes [39].

Wang et al. [40] reviewed the relevant previous studies and found that the highest emission concentrations occurred in the following situations: (1) peat, wood, and raw coal were used in stoves; (2) olive oil was used; (3) high temperature cooking; (4) without clean technology. The concentrations of particulate matter and VOCs emitted from cooking were 0.14–24.46 mg/cm^3 and 0.35–3.41 mg/m^3, respectively. The content of gaseous pollutants will increase greatly due to incomplete combustion or low combustion efficiency. Zhao et al. [41] analyzed the characteristics of cooking oil fume pollutants according to different influencing factors and found that the cooking method is probably the main factor in the emission of pollutants in Chinese cooking. The air pollutants from oil-based cooking are much higher than those from water-based cooking, and a gas stove will release more pollutants than an electric stove. Although there have been extensive studies on the

concentration values of pollutant emissions, they mainly focus on the peak or average values. Besides, the investigation of the entire cooking process is still very lacking, including the preheating of the pot and oil and the cooking process after the ingredients have been added to the pot. In order to better understand the emission characteristics of cooking oil fume and achieve higher removal efficiency, the relevant research needs to be strengthened and improved.

Table 1. VOC emission concentrations in different types of cuisine.

| Cuisine	VOC Emission Concentration/$\mu g \cdot m^{-3}$	References
Barbecue	3494 ± 1042	
Hunan cuisine	494.3 ± 288.8	[36]
Home cooking	487.2 ± 139.5	
Shandong cuisine	257.5 ± 98.0	
Barbecue	12,470.6	
Huaiyang Cuisine	2965.9	
Cantonese	2297.1	
Shandong cuisine	2233.3	[37]
Home cooking	1843.1	
Sichuan cuisine	1827.9	
Hunan cuisine	1827.9	
Barbecue	12,219.5	
Chinese food	4283.2	[38]
Sichuan cuisine	5445.7	
Zhejiang cuisine	3925.1	
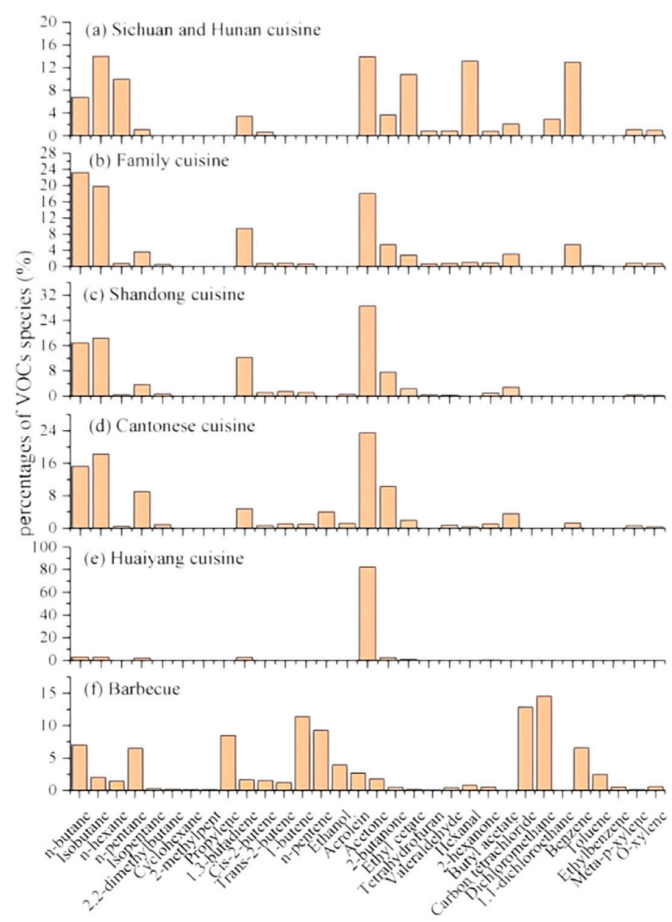
Figure 3. VOC mass concentration percentage in various types of cuisine [37].

From the above results, it can be seen that different oils, temperatures, and cuisines will affect the emission characteristics of cooking oil fume. Different oils differ in the

content and type of fatty acids. In general, unsaturated fatty acids, rich in double bonds, are more easily oxidized than saturated fatty acids, producing more aldehydes, alkanes, and olefins, which cause vegetable oils that are rich in unsaturated fatty acids to release more VOCs than lard. Temperature is an important factor affecting physicochemical reactions. As the temperature increases, the rate of fatty acid decomposition increases significantly, volatilizing higher organic compounds and boiling points, leading to an increase in the concentration and composition of VOCs. Among these, the main components are aldehydes, olefins, and alkanes, which account for more than half of the total detected VOC concentrations. The cuisine and cooking style also affect the emission of cooking fumes. The emission concentrations from grilled cuisines were significantly higher than those from non-grilled cuisines; the VOCs emitted from grilled cuisines consisted mostly of hydrocarbons. In contrast, non-grilled cuisines have an increased content of alcohols, which, together with alkanes and aldehydes, constitute the main pollutants. Compared to foreign countries, the variety of cooking styles in China leads to higher concentrations of cooking oil fumes in the kitchen.

3. Comparison of Various Purification Methods

In view of the great harm caused to the environment and humans by cooking oil fumes, the effective removal of cooking oil fumes has become an urgent problem. Various purification methods have been studied and are commonly divided into physical capture, chemical decomposition, and combination methods [42]. Their technical characteristics are summarized in Table 2.

3.1. Physical Capture Methods

The physical capture methods mainly focus on the removal of particulate matter, which includes mechanical separation, filtration, adsorption, washing absorption, and the electrostatic deposition method.

Mechanical separation is a typical physical treatment method, divided into inertial, gravity, and centrifugal separation [43–45]. The inertial separation method changes the airflow direction by setting up folded plates and filters to make the oil droplets collide and stick to the pipe. Gravity and centrifugal separation methods use gravity and centrifugal force, respectively. The mechanical separation method has a simple structure and low investment and operating costs. Due to its low purification efficiency, it is often used in situations with low processing requirements or as pretreatment in combination with other technologies [46,47].

The filtration-adsorption method utilizes the characteristics of a large specific surface area ratio, high surface energy, and strong adsorption of the adsorption medium to absorb the pollutants. Porous materials such as activated carbon and molecular sieves are typically used [48,49]. This method is simple, inexpensive, and suitable for treating low to medium concentrations of oil fume waste gas. However, the filter media clogs easily and needs to be replaced regularly, and the treatment of the filter media may cause secondary pollution [50,51].

The washing absorption method is a wet treatment process that converts pollutants into the liquid phase through full contact with the absorption solution [52,53]. According to the different gas-liquid contact methods, they can be divided into types of liquid membrane, spray, and impact. This method requires a large absorbent solution and may produce secondary pollution. It can remove some irritating odors and is suitable for treating oil fumes because of its simple composition and high water solubility [54,55].

In contrast, the electrostatic deposition method uses the ionization of cooking oil fume in a high-voltage electric field to charge particulates, which move towards the dust collection pole under the action of the electric field force and finally deposit to purify the fume [56–59]. This method has a small footprint, is highly efficient, and is widely used. However, long-term use will lead to the formation of an oil film on the electrode surface, which will affect the purification efficiency and pose a potential fire hazard.

3.2. Chemical Decomposition Methods

Chemical decomposition methods focus on removing VOCs by oxidizing and breaking them down into CO_2, H_2O, and other non-toxic small molecules. Table 2 includes the methods of thermal oxygen incineration, catalytic combustion, low-temperature plasma, photolysis, catalytic oxidation, and biodegradation.

Figure 4 shows the schematic diagram of the three related purification methods: (a) thermal oxygen incineration; (b) catalytic combustion; (c) low-temperature plasma. In the thermal oxygen incineration method, the VOCs are completely oxidized at high temperatures, and there is no visible flame due to the low concentration of VOCs [60,61]. This method has high efficiency in removing oil fumes and odors, but the energy consumption and cost are quite high, and it is less used [62,63]. In order to decrease the oxidation temperature of VOCs, catalytic combustion is conducted by adding catalysts to reduce the activation energy of decomposing VOCs [64–66]. It is considered one of the most promising methods for treating cooking oil fume due to the advantages of high efficiency and environmental protection [67,68]. The development of efficient and low-temperature catalysts for catalytic combustion is a difficult and hot topic at present.
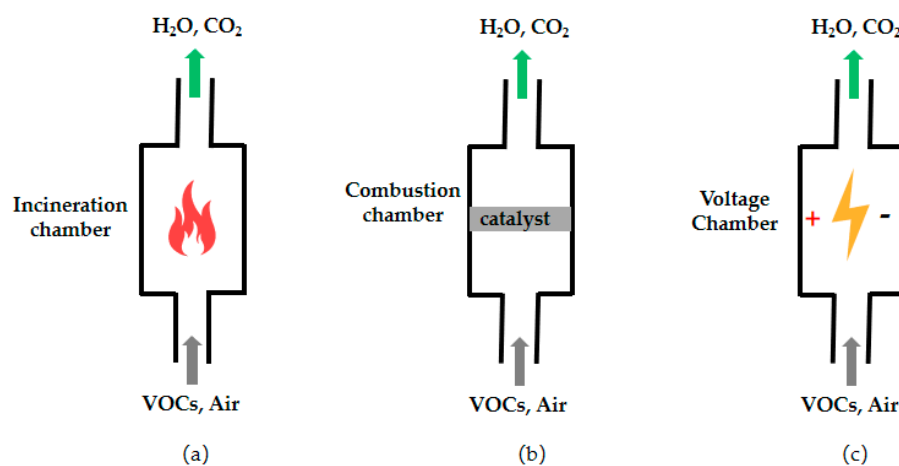

Figure 4. Schematic diagram of the three related purification methods: (**a**) thermal oxygen incineration; (**b**) catalytic combustion; (**c**) low-temperature plasma.

Low-temperature plasma methods can remove the pollutants by instantaneous high-frequency discharge to decompose VOCs into harmless molecules or generate high-energy electrons and reactive radicals to react with the VOCs [69–71]. The low-temperature plasma method is a cross-integrated technology that integrates physics, chemistry, and environmental science with strong purification and sterilization abilities [72,73]. However, its high cost and the danger of treating flammable and explosive waste gases limit its application. Photolytic oxidation gradually oxidizes VOCs into low-molecular-weight intermediates and eventually generates H_2O and CO_2 under exposure to ultraviolet light [74–76]. Catalysts (such as titanium dioxide, zirconium dioxide, and other semiconductor materials) are also used to perform photocatalytic oxidation reactions to improve the purification efficiency. The method is simple to operate and has a long service life. However, it can only be applied to the treatment of low concentrations of oil fume exhaust gases due to its low utilization rate of light energy and unstable purification effect [77,78].

As a biochemical method, the biodegradation method uses the metabolic activities of microorganisms to convert harmful substances into small inorganic molecules [79–82]. Although the method has low operating costs and can effectively avoid secondary pollution, it has not been widely applied because of its unstable working conditions and long time consumption.

Combined with the analysis in the table, it can be seen that the physical capture methods remove particulate matter more efficiently than VOCs. In contrast, chemical decomposition methods cannot effectively remove particulate matter but have a high

removal efficiency for VOCs. The use of different purification methods should be reasonably selected according to the actual needs.

3.3. Combination Methods

Compared to a single treatment method, combination methods can remove pollutants more efficiently due to the complex components of cooking oil fume [83–92]. The combination method combines two or more individual methods to take advantage of their strengths. For example, the combination of electrostatic deposition and washing absorption methods can efficiently purify total cooking fume pollutants due to their effective removal capacities for VOCs and particulate matter, respectively. Although the mechanical centrifugation method has low purification efficiency, it can be used as a pre-treatment step to reduce the back-end pressure. With electrostatic deposition, filtration, and adsorption methods, particulates in cooking oil fume can be effectively removed [93]. Maciuca et al. [94] used a combination of low-temperature plasma and photocatalysis to study the synergistic effect of the oxidation of isovaleraldehyde at low concentrations. The result showed that the removal efficiencies of isovaleraldehyde by photocatalysis and low-temperature plasma methods were about 33% and 40%, respectively, while the purification efficiency could reach 85% with the combination method. He et al. [95] studied integrated biotrickling filtration (BTF) and photocatalytic oxidation (PCO) systems for treating organic waste gas. The study found that the high-concentration and multicomponent VOCs were removed effectively and in an environmentally friendly manner. It has been shown that by coupling multiple methods, the advantages of various VOC purification methods can be fully exploited in order to achieve efficient degradation.

Table 2. Characteristics of cooking oil fume pollutant purification methods.

Purification Method		Advantage	Shortcoming	Particulate Matter Removal Rate	VOC Removal Rate	Cost	Application Area	References
Physical capture methods	Mechanical separation	Simple structure and low cost	Low efficiency and frequent cleaning	Medium	—	Low	Pretreatment and low-demand	[43–47]
	Filter adsorption	Easy operation and maintenance	Easily clogged by filter materials	Medium	Low	Low	Medium and low concentrations of exhaust gas	[48–51]
	Washing absorption method	Easy management and stable operation	High consumption of absorbing liquid, with secondary pollution	Low	Medium	Medium	Suitable for simple ingredients and high water solubility	[52–55]
	Electrostatic deposition	Compact equipment, wide range of applications	Reduced efficiency and fire hazards after long-term use	High	Low	Medium	Widely used due to its high efficiency and mature technology	[56–59]
Chemical decomposition methods	Thermal Oxygen Incineration	High efficiency and effective odor removal	High energy consumption and cost	—	High	High	High cost of installation and less use	[60–63]
	Catalytic combustion	Thorough treatment and effective odor removal	High cost and regular replacement of catalyst	—	High	Medium	A wide range of applications	[64–68]
	Low-temperature plasma method	The equipment is compact, safe, and efficient	High cost and danger of treating flammable waste gases	—	High	High	Large catering units with higher requirements	[69–73]
	Photolysis oxidation	Simple operation and long service life	Low utilization of light energy and an unstable effect	—	Low	Medium	Exhaust gas with low concentration and small airflow	[74–78]
	Biodegradation	Low cost and environmental protection	Unstable working state and long degradation time	—	Medium	Medium	Appropriate environment and stable working conditions	[79–82]

Table 2. *Cont.*

Purification Method		Advantage	Shortcoming	Particulate Matter Removal Rate	VOC Removal Rate	Cost	Application Area	References
Combination methods	Mechanical separation and electrostatic deposition	Effective removal of particulate matter	Low removal efficiency of VOCs	High	Low	Medium	Suitable for efficient removal of particulate matter	[93]
	Low-temperature plasma and photocatalysis	High removal efficiency of VOCs	High cost	—	High	High	Suitable for high removal requirements of VOCs	[94]
	Biotrickling filtration and photocatalysis	Effective removal of cooking oil fumes	Unstable working conditions	Medium	High	Medium	Suitable for removing the pollutants in cooking oil fumes	[95]

4. Catalytic Combustion of VOCs

Among the various removal methods of cooking oil fume, the catalytic combustion method is a promising technology due to its high efficiency and low secondary pollution. The efficiency is generally above 90%, and the final products are CO_2 and H_2O, which basically do not cause secondary pollution. The cooking oil fume is completely oxidized by the typical gas-solid phase catalytic reaction, where the catalyst could lower the activation energy and enrich the reactant molecules on the surface of the catalyst sites to increase the reaction rate. Due to the effect of catalysts, the VOCs undergo flameless combustion at low light-off temperatures. To promote the efficiency of the removal, the catalytic mechanisms, effects of cooking oil fume components, and various catalysts were analyzed and summarized as below.

4.1. Mechanisms of Catalytic Combustion

Although the catalytic oxidation of VOCs in cooking oil fumes has been widely studied, it is difficult to propose a single reaction mechanism due to the different properties of pollutants, catalysts, and reaction conditions. Three types of catalytic oxidation are commonly used to explain the process: the Marse-van Krevelen (MVK) mechanism, the Langmuir-Hinshelwood (L-H) mechanism, and the Eley-Rideal (E-R) mechanism [96–111]. Relevant studies that applied different catalytic oxidation mechanisms are listed in Table 3.

Table 3. Application of different catalytic oxidation mechanisms.

VOC	Catalyst	Mechanism	References
Methyl ethyl ketone	Cr/ZrO_2	Marsevan Krevelen	[104]
n-hexane	Pt/Al_2O_3	Marsevan Krevelen	[105]
Propane	$Mn/ClayM$	Marsevan Krevelen	[106]
Toluene	$Co_{.6}Al_{1.2}Ce_{0.8}$ HT500	Marsevan Krevelen	[107]
Propylene	$Pd-Au/TiO_2$	Langmuir-Hinshelwood	[108]
Toluene	$Cu_{0.13}Ce_{0.87}O_y$	Langmuir-Hinshelwood	[109]
Trichloroethylene	Pd/Al_2O_3	Eley-Rideal	[110]
Cyclooctane	$Pt/\gamma-Al_2O_3$	Eley-Rideal	[111]

The MVK mechanism, also called the redox mechanism since the catalyst is first reduced and then oxidized in the reaction process, has been widely used in the field of catalytic oxidation. It is assumed that the reaction occurs between the adsorbed VOCs and the lattice oxygen of the catalyst. The process is divided into two steps: VOCs first react with lattice oxygen to reduce the metal oxide, and then the reduced metal oxides are re-oxidized by gas-phase oxygen [112]. Li et al. [113] prepared a 7% $CuO/Ce_{1-x}Mn_xO_2$ catalyst for the catalytic oxidation of benzene, and the reaction paths are shown in Figure 5a. Three different paths exist in this reaction: path (i): $Ce_{1-x}Mn_xO_2$ releases oxygen species, then adsorbs and oxidizes benzene; path (ii): CuO can also release oxygen species, then

adsorb and oxidize benzene; path (iii): benzene is adsorbed by CuO and oxidized by the oxygen species released by $Ce_{1-x}Mn_xO_2$. The redox interaction between CuO and $Ce_{1-x}Mn_xO_2$ enabled the catalyst to obtain high activity similar to that of noble metals. In the current field of catalytic oxidation, the MVK mechanism is commonly used to describe the catalytic oxidation process of VOCs.

L-H is a heterogeneous catalytic mechanism based on the principles of adsorption and desorption, and the reaction is believed to occur between adsorbed VOCs and adsorbed oxygen [114]. It can be divided into single-site L-H and double-site L-H mechanisms according to whether oxygen and VOCs are adsorbed on the same active site. Using the example of the catalytic combustion of Pd-Au/TiO$_2$ catalyst to purify toluene [108]. The L-H mechanism dominates the oxidation process, and the specific reaction path is shown in Figure 5b. VOCs (toluene) are adsorbed on the active sites of the Pd-Au/TiO$_2$ catalyst and undergo catalytic oxidation with the oxygen species adsorbed on the catalyst surface to generate CO_2 and H_2O. The oxidation products are finally desorbed from the catalyst surface and returned to the gas phase. In the L-H mechanism, the adsorbed molecules react on the catalyst surface and then re-enter the gas phase when their thermal motion is sufficient to overcome the energy barrier of the adsorbent gravitational field, in which the reaction rates of adsorption and desorption can reach dynamic equilibrium during the whole reaction.

In the E-R mechanism, VOCs in the gas phase react with adsorbed oxygen on the catalyst surface, which is the main control step in the entire catalytic oxidation process [115]. Burgos et al. [116] prepared Pt/Al$_2$O$_3$ catalysts for the catalytic oxidation of toluene, and the reaction mechanism was derived by combining TPD and TPSO experiments, as shown in Figure 5c. The reaction process is as follows: oxygen species are first chemisorbed on Pt, and then toluene is catalytically oxidized in the gas phase. The E-R mechanism is different from the MVK and L-H mechanisms; the catalytic oxidation reaction is minimally affected by competing adsorption since the VOCs can react with the oxygen component directly in the gas phase.
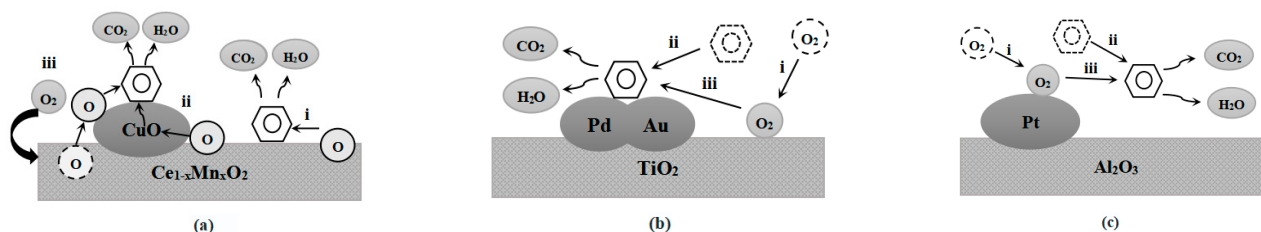

Figure 5. (**a**) Mechanism of benzene oxidation over CuO/$Ce_{1-x}Mn_xO_2$ catalysts [113]; (**b**) Mechanism of benzene oxidation over Pd-Au/TiO$_2$ catalyst [108]; (**c**) Mechanism of benzene oxidation over Pt/Al$_2$O$_3$ catalyst [116].

Although the adsorption patterns of VOCs and oxygen species in the MVK, L-H, and E-R mechanisms are different, the basic reaction pathway can be attributed to the fact that VOCs in the gas phase enter the catalyst surface through internal and external diffusion and are finally oxidized to CO_2 and H_2O by the gas-adsorbed oxygen or the lattice oxygen of the catalyst. Then the generated CO_2 and H_2O are desorbed from the catalyst surface and returned to the gas phase through diffusion, while the continuously introduced O_2 in the gas phase fills the oxygen vacancies or adsorbed reactive oxygen species on the catalyst surface and finally achieves a complete redox cycle of adsorption, oxygen depletion, desorption, and oxygen replenishment.

4.2. Effects of Different Model Compounds

The overall degradation of cooking oil fumes is quite difficult due to the complex composition and different properties of VOCs. Most of the experiments select representative model compounds to compare the catalytic performances and effects of different compo-

nents. These model compounds, tested under different catalysts and reaction conditions, are listed in Table 4.

4.2.1. Aliphatic Hydrocarbons

The most abundant VOCs in cooking oil fume are hydrocarbon compounds, including alkanes such as n-pentane, n-heptane, and n-hexane and olefins such as octene and heptene [117–119]. Diaz et al. [120] used n-hexane as the model compound of cooking oil fume. They prepared a series of $Mn_{1-x}Ce_x$ (x = 0, 0.05, 0.1, 0.2, and 1) catalysts by ultrasonic impregnation for the catalytic oxidation reaction at 330 °C. It was found that the total combustion sequence of n-hexane is as follows: $Mn_1Ce_0 \approx Mn_{0.9}Ce_{0.1} > Mn_{0.95}Ce_{0.05} > Mn_{0.8}Ce_{0.2} \gg Mn_0Ce_1$. Mn_1Ce_0 and $Mn_{0.9}Ce_{0.1}$ performed the highest catalytic activity of almost 100% conversion. However, the Mn_1Ce_0 showed worse catalytic stability than the $Mn_{0.9}Ce_{0.1}$. The latter maintained high activity after a 34 h reaction, while the former remarkably decreased by 30% after a 17 h reaction at 250 °C. The addition of Ce to the Mn catalyst did not improve its activity, but it could improve catalytic stability. After TPR and XPS detection, it was proven that the excellent catalytic activity and stability were attributed to the interaction between Mn and Ce by forming Mn-Ce solid solutions, which kept Mn in the oxidized state. Ousmane et al. [121] used propylene as the model compound and prepared noble metal-supported catalysts with Au and four different carriers (CeO_2, TiO_2, Al_2O_3, and $7.5Ce/Al_2O_3$). The result indicated that Au/CeO_2 had the highest catalytic activity due to the high dispersion of Au on the CeO_2 carrier, which could completely oxidize propylene at 210 °C. While $7.5Ce/Al_2O_3$, TiO_2, and Al_2O_3 were used as carriers, the complete conversion temperatures of propylene were 250 °C, 315 °C, and 325 °C. It can be seen that the dispersibility of the active components on the carrier and the interaction between them have an important influence on the catalytic performance.

4.2.2. Ketone Aldehydes

Ketone aldehydes, as the second highest component in cooking oil fume (about 20–30%), mainly contain acetone, butanal, hexanal, etc. They have different properties for containing oxygen functional groups [122,123]. Mitsui et al. [124] investigated the catalytic combustion of acetaldehyde over various oxide-supported metal catalysts prepared by the impregnation method. It was found that SnO_2-supported noble metal catalysts showed the highest activity, as the 90% conversion temperature (T_{90}) of acetaldehyde was 180 °C. This was because supported Pt particles were highly dispersed on SnO_2. Zhu et al. [125] studied the catalytic oxidation of low-concentration acetone with a novel multilayer MnO_x/TiO_2 composite nanofiber prepared by electrospinning technology and a hydrothermal growth method. The catalyst with 30% Mn content showed the best performance (T_{90} = 290 °C), which is attributed to the special stacked morphology of the nanofiber, its large specific surface area, and the abundant surface adsorption of oxygen.

4.2.3. Aromatic Hydrocarbons

Although aromatic compounds have a small proportion in cooking oil fume, they are potent carcinogens and seriously threaten human health, which has received widespread attention in recent years [126,127]. Zhang et al. [128] selected toluene as a model component and prepared a MnO_2-loaded single-atom Pt catalyst using a one-step hydrothermal method. It turned out that a single Pt atom could significantly enhance the surface oxygen activity and form hydroxyl radicals (•OH), which improved the catalytic activity for toluene degradation at room temperature. A low concentration of toluene (0.42 ppm) could be completely removed at 28 °C under high space velocity conditions. Besides, the experiment achieved 100% conversion of 10 ppm toluene at 80 °C and complete oxidation to CO_2 and H_2O at 220 °C. This research provides a reference for low-temperature catalytic purification of aromatic hydrocarbon types of VOCs in practical applications.

4.2.4. Mixed Component of VOCs

In view of the complex components of cooking oil fume, catalytic oxidation of mixed components of VOCs has also been studied [129,130]. Zhao et al. [131] used the mixture of toluene and ethyl acetate as the model component for VOCs and prepared a series of cordierite-supported Co-Mn composite oxide monolithic catalysts by ultrasonic impregnation. The supported Mn could effectively control the Co_3O_4 spinel structure to form a solid solution. The $Co_{0.67}Mn_{0.33}O_x$ catalyst had high catalytic activity, so the mixed pollutants toluene and ethyl acetate could be catalytically decomposed into CO_2 and H_2O at 230 °C. XPS and TPR characterization found that the high activity of the catalyst was related to the formation of Co-Mn solid solution, abundant surface adsorbed oxygen, and Co^{3+} and Mn^{3+} species. The 90% conversion temperature (T_{90}) of toluene in the mixed pollutants was 225 °C, which was lower than that of single component toluene (T_{90} = 237 °C). While the ethyl acetate in the mixture (T_{90} = 237 °C) was 6 °C higher than that of the single-component. The competitive adsorption of toluene and ethyl acetate on the catalyst may cause this. Research showed that the total degradation efficiency of mixed pollutants was related to the properties of the pollutant components, and the complete conversion temperature mainly depended on the part that was more difficult to degrade [132]. Studies have also shown an impact on the reaction path between the mixed components of VOCs in addition to competitive adsorption [133]. The catalytic oxidation of o-xylene and its mixed components with isopropanol was investigated using an acidic zeolite (HY) catalyst. The addition of isopropanol was found to promote the oxidation of o-xylene. The reason was that isopropanol could be converted to propylene and then reacted with o-xylene to form isopropyldimethylbenzene, which could be more easily oxidized.

Table 4. Catalytic combustion method for the degradation of different model compounds.

Catalyst	Preparation	VOC	Concentration (ppm)	Space Velocity (h^{-1})	Temp (°C)	Conversion (%)	References
$Mn_{0.9}Ce_{0.1}$	Impregnation	n-hexane	—	11,000	330	100	[120]
Au/CeO_2	Precipitation	Acrylic	1000	35,000	210	100	[121]
Pt/SnO_2	Impregnation	acetaldehyde	—	10,000	180	90	[124]
MnO_x/TiO_2	Electrospinning-Hydrothermal Synthesis	Acetone	500	360,000	290	90	[125]
Pt/MnO_2 (single atom)	One-step hydrothermal	Toluene	10	60,000	220	100	[128]
$Co_{0.67}Mn_{0.33}O_x$	Impregnation	Toluene, ethyl acetate	500	45,000	230	100	[131]

4.3. Effects of Catalysts

As a crucial part of the catalytic combustion method, preparing more efficient, environmentally friendly, and stable catalysts has become a hot research topic. The commonly used catalysts are mainly divided into two categories: noble metal catalysts and non-noble metal oxide catalysts. Related studies are summarized in Tables 5 and 6.

4.3.1. Noble Metal Catalysts

Noble metals mainly include gold, silver, and platinum group metals (platinum, palladium, rhodium, ruthenium, osmium, and iridium), which have excellent low-temperature catalytic oxidation activity due to strong adsorption and electron transfer ability caused by the vacancy of the d electron orbital. However, noble metals are expensive and unstable at high temperatures. They are prone to lose activity due to aggregation and sintering. So, noble metals are usually supported on carriers to form a supported catalyst so that the noble metal can be uniformly dispersed on the surface of the catalyst, which is beneficial to improve the catalytic activity and reduce the cost [134–137]. Noble metal catalysts for catalytic purification of VOCs are summarized in Table 5.

Low cost and high specificity surface material carriers, such as γ-Al_2O_3, SiO_2, TiO_2, CeO_2, molecular sieves, and composite carriers, are commonly used. The dispersing effects of various carriers on the noble metals (such as Au, Pt, and Pd) are different. Ousmane et al. [121] selected different supports (CeO_2, Al_2O_3, and TiO_2) and prepared a series of supported Au catalysts by the deposition precipitation method. Experiments showed that the Au/CeO_2 catalyst had the best activity and could convert propylene completely at 230 °C. As shown in Figure 6, the Au particles on CeO_2 carriers are only 3–5 nm in size, more dispersive than other carriers, and therefore perform the highest catalytic activity. It shows that the dispersion of the active component on the carrier is closely related to the activity of the catalyst. Carabineiro et al. [138] also prepared supported Au catalysts with different oxide supports (CuO, Fe_2O_3, La_2O_3, MgO, NiO, and Y_2O_3). They found that Au/CuO had the highest catalytic activity, which could convert 90% of ethyl acetate at 272 °C and almost completely oxidize at 289 °C. Due to the reducibility of the CuO and the suitable size of the gold nanoparticles, this catalyst could promote the exchange between lattice oxygen and surface oxygen, thus improving the catalytic oxidation performance. In addition, due to the complex components of cooking oil fume, the overall degradation of VOCs has been studied in addition to the single-component [139–142]. Wang et al. [139] prepared monolithic catalysts with Pt and different carriers (γ-Al_2O_3, La-Al_2O_3, and YSZ-Al_2O_3). Their results showed that the Pt/La-Al_2O_3 catalyst had the highest activity, as the cooking oil fume removal rate could reach 90% at 350 °C. This is because the crystal of La-Al_2O_3 is a sub-crystal, resulting in more active atoms and highly dispersed Pt atoms on the carrier. Besides, the Pt/La-Al_2O_3 catalyst had a lower conversion temperature and a wider operation range than GHSV, which showed great potential for application.
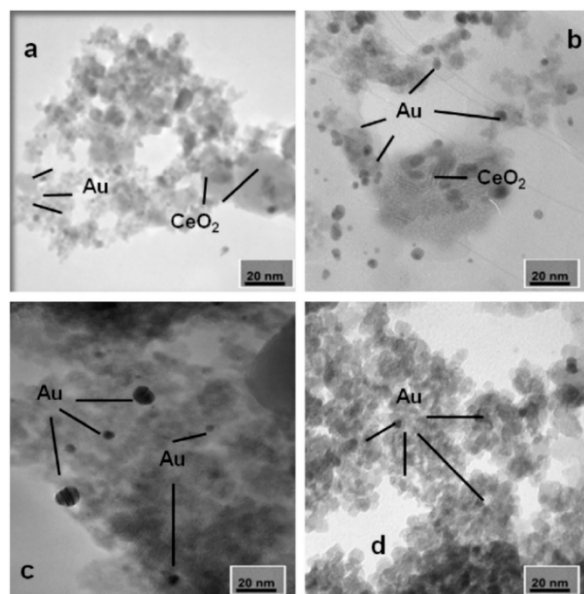

Figure 6. TEM of Au on different supports: (**a**) Au/CeO_2; (**b**) $Au/Ce_{7.5}/Al_2O_3$; (**c**) Au/Al_2O_3; (**d**) Au/TiO_2 [121].

The activity of catalysts can also be improved by adding suitable additives. Sedjame et al. [143] prepared CeO_2-Al_2O_3-supported Pt catalysts with different loadings of Ce (0, 7, 15, 23, and 51 wt%) by the sol-gel method. The addition of ceria to alumina led to modifications in the physical and chemical properties of the material, thus affecting the catalytic performance. The activity of catalysts with different Ce loadings (0, 7, 15, and 23 wt%) was evaluated with n-butanol, and the temperatures of 50% conversion rate (T_{50}) were 143 °C, 158 °C, 157 °C, and 138 °C. Although ceria covers the alumina surface and reduces the specific surface area, the oxygen storage capacity of the material is also enhanced. This resulted in higher or lower catalytic activity for catalysts with different Ce additions than those without Ce. Barakat et al. [144] prepared Pd-CeO_2/TiO_2 (0.5 wt% and

5 wt% Ce) catalysts to investigate the influence of CeO_2. The TEM results showed that a 0.5 wt% Ce catalyst had a lower BET surface area and larger TiO_2 crystallites than a 5 wt% Ce catalyst. This was proven by UV-visible and TPR experiments. These results indicated CeO_2 could produce Pd particles with higher dispersion and smaller size for improved catalytic performance.

Not just the carriers, but the kinds of noble metals are also key factors. Huang et al. [145] compared the catalytic activity of γ-Al_2O_3 supported different noble metals (Pd, Pt, Au, Ag, and Rh) catalysts and discovered that 1 wt% Pd/Al_2O_3 catalyst had the highest activity. It could completely oxidize 100 ppm o-xylene at 110 °C. A two-path reaction mechanism in the catalytic reaction was proposed, as shown in Figure 7. In pathway I, the adsorbed o-xylene molecules were oxidized to benzyl alcohol species and then generated 2-methyl benzaldehyde, 1(3H)-isobenzofuranone, or phthalate via rapid oxidation. The 2-methyl benzaldehyde and 1(3H)-isobenzofuranone could be further oxidized to phthalate species to generate surface maleate. Then the adsorbed maleate species were oxidized to the surface carboxylate (formate/acetate) species and finally converted to CO_2 and H_2O. In pathway II, the o-xylene molecules adsorbed on the metallic Pd were oxidized directly into CO_2 and H_2O through the interaction between the adsorbed o-xylene and oxygen. This reaction occurs between the adsorbed VOCs and the adsorbed oxygen, which is consistent with the process in the L-H mechanism. Studies showed that the carrier also had certain catalytic activity for VOCs, which could improve the total conversion rate of the reaction. The overall performance of the catalyst can be improved by selecting a suitable carrier during the preparation process.
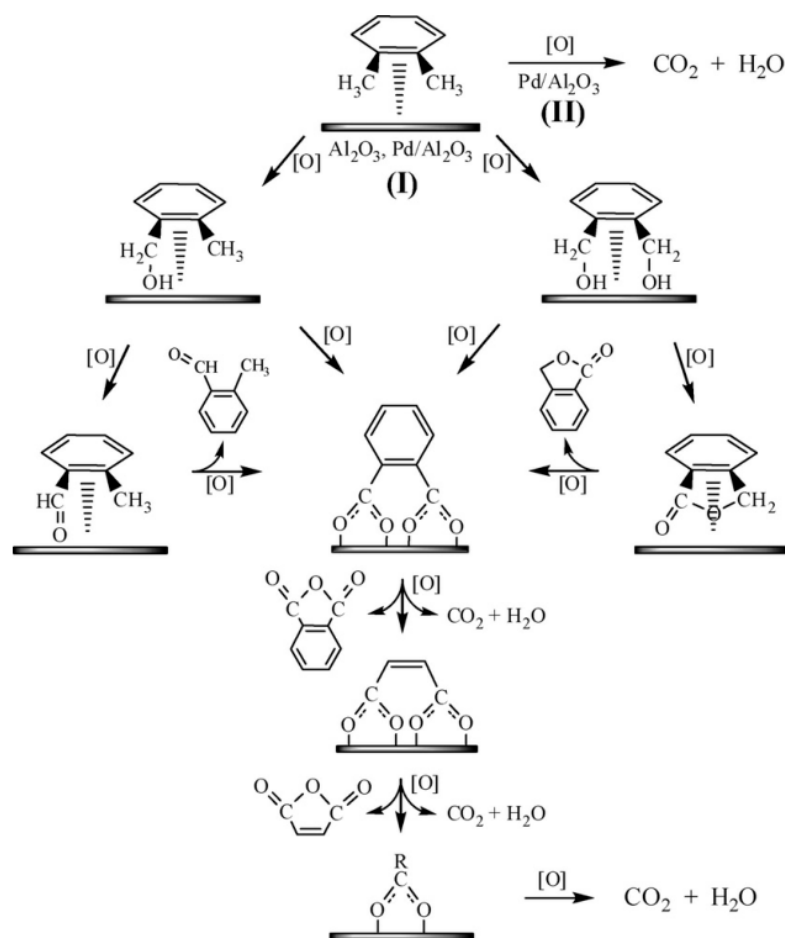

Figure 7. Reaction path diagram for the catalytic oxidation of o-xylene over Pd/Al_2O_3 catalyst [145].

Table 5. Noble metal catalysts for catalytic oxidation of VOCs.

Catalyst	Preparation	VOC	Concentration (ppm)	Space Velocity (h^{-1})	Temp (°C)	Conversion (%)	References
Au/CeO_2	precipitation	Acrylic	1000	35,000	230	100	[121]
Au-CuO	Double impregnation	Ethyl acetate	466.7	60,000	272	90	[138]
$Pt/La-Al_2O_3$	Impregnation	Oil fume	—	10,000	350	90	[139]
$Pd/La-Al_2O_3$	Impregnation	Oil fume	—	10,000	400	78	[139]
$Pt+Pd/La-Al_2O_3$	Impregnation	Oil fume	—	10,000	350	86	[139]
$Pt/\gamma-Al_2O_3/Ce_{0.4}Zr_{0.4}Mn_{0.2}O_2$	Impregnation	Oil fume	—	10,000	222	90	[140]
$Pt/La-Al_2O_3+Pt/OSM$	Impregnation	Oil fume	—	10,000	270	100	[141]
Pt/CNT	Impregnation	Oil fume	—	5700	300	90.4	[142]
$Pt/CeO_2 -Al_2O_3$	Sol-gel	n-butanol	1000	60,000	167	90	[143]
$Pd-CeO_2/TiO_2$	Impregnation	Toluene	1000	—	220	90	[144]
Pd/Al_2O_3	Impregnation	O-xylene	100	10,000	110	100	[145]

Noble metal catalysts have excellent low-temperature catalytic performance for most VOCs, but they are expensive and easily deactivated at high temperatures. To further improve the activity and economy of noble metal catalysts, preparing carriers with higher-specific surfaces and adding suitable catalyst additives should be considered.

4.3.2. Non-Noble Metal Catalysts

Compared with noble metal catalysts, non-noble metal catalysts have the advantages of abundant sources and low prices [146–148]. In particular, transition metals have been extensively studied in recent years due to their high activity and economy. Non-noble metal catalysts can be mainly divided into single metal and composite metal catalysts, while the composite metal catalysts include perovskite, spinel, and other composite catalysts. Non-noble metal catalysts for catalytic purification of VOCs are summarized in Table 6.

(1)   **Single metal catalysts**

Chen et al. [149] prepared oxides of Co, Cu, Fe, La, and Ni by an external template method that used carbon xerogel (CX) and activated carbon (AC) as template agents. Both of the two teasing agents could improve the specific surface area. Among them, carbon dry gel was a better template material than activated carbon to produce more active oxides. Co_3O_4 prepared with carbon xerogel as a template had a large specific surface area and strong reducing properties. It showed high catalytic activity towards ethyl acetate, and the conversion rate reached almost 100% at 245 °C. Lin et al. [150] studied the catalytic oxidation performance of acetone over an aluminosilicate-supported Ce catalyst. It found both the redox capacity and surface acidity were important factors affecting the catalytic performance. The acidity could improve the catalytic oxidation of acetone but also cause the rapid formation of coke to deactivate the catalyst. Therefore, the surface acidity of the catalyst should be controlled in the appropriate range considering the catalytic activity and stability. Yi et al. [151] studied the catalytic performance of different MnO_2-supported cordierite catalysts on cooking oil fume. It was found that the Mn content and calcination temperature of catalysts had a great influence on the catalytic oxidation performance of non-methane hydrocarbons (NMHC). The MnO_2/cordierite catalyst with 5% Mn loading and prepared at the calcination temperature of 400 °C showed the best catalytic activity due to the good pore structure and MnO_2 dispersion.

(2)   **Composite metal catalysts**

Composite metal catalysts mainly include perovskite, spinel, and other composite catalysts. Compared to single metal catalysts, the interaction between metals in composite metal catalysts can further enhance the performance of the catalyst.

Perovskite catalysts

Perovskite is a composite oxide with the general formula ABO_3. The A-site ion is generally a rare earth or an alkaline earth ion with a tetrahedral structure, which can maintain the stability of the crystal. The B-site ion is the main active source of the catalyst

and is generally a transition metal ion with an octahedral structure [152–154]. Perovskite catalysts are inexpensive, stable, and have good catalytic performance, which has resulted in their widespread use in the catalytic purification of VOCs. The most commonly used are lanthanum-based perovskites, such as $LaMnO_3$ and $LaCoO_3$ [155,156].

Blasin-Aubé et al. [157] studied the catalytic oxidation of various VOCs over $La_{0.8}Sr_{0.2}MnO_{3+x}$ perovskite catalysts. All the VOCs (ethyl acetate, hexane, toluene, and acetone) in the experiment were completely converted to CO_2 and H_2O at temperatures below 350 °C. It turned out that the strength of the weakest C-H bond in the structure was the main factor in determining the reactivity of the hydrocarbons in the oxidation reaction, but for the oxygenated compounds, this argument could not be applied. The study found that it was quite difficult to discover the general rules even when a parameter, such as a catalyst or components of the mixture, was fixed. For the mixtures, each composition must be studied in order to determine its behavior with the catalyst. This is also a difficult area for removing cooking oil fumes and requires the development of efficient catalysts. Alvarez-Galvan et al. [158] added K to $LaMnO_3$ to prepare the $La_{0.9}K_{0.1}MnO_3$ catalyst. The research revealed that the catalyst had high catalytic activity for butanone, and the complete conversion temperature was 267 °C. The increase in specific surface area, Mn^{4+}, and reactive oxygen species after K doping were the main factors for improving catalyst activity. The preparation method can affect the specific surface area and crystallinity, resulting in different catalytic activities. A $La_{0.9}Ce_{0.1}CoO_{3\pm\delta}$ perovskite has been prepared by a new flame-hydrolysis (FH) method [159]. As a result, the catalyst has a high crystallinity, surface area, and thermal resistance. The TPD-MS results showed that the $La_{0.9}Ce_{0.1}CoO_{3\pm\delta}$ catalyst had quick oxygen transport through the perovskitic lattice and good redox properties. This new method of preparing catalysts was useful for practical application in the environmentally friendly catalytic combustion of methane and provided a reference for removing other VOCs.

Spinel catalysts

Spinel is commonly represented by AB_2O_4 as an important structure type of complex oxide. The A and B site ions are located at the center of the regular tetrahedron and octahedron. The active components of spinel catalysts are mainly transition metals with good catalytic activity, such as Cu, Mn, and Co [160–162]. Spinel catalysts have a good catalytic oxidation effect on hydrocarbons, especially at low temperatures, which favors low-temperature catalytic combustion of VOCs [163–165].

Zavyalova et al. [166] prepared spinel-structured AB_2O_4 catalysts (A = Co, Cu, B = Cr, Co) by the gel-combustion method and used them in the catalytic oxidation of n-hexane. Results showed that the $CuCo_2O_4/CeO_2$ catalyst with high dispersion of the active components had the highest activity and could completely remove n-hexane at 280 °C. Previous studies have shown that the activity of surface A ions in octahedral positions greatly exceeds that of A ions in tetrahedral positions. The synergistic effect between copper and cobalt metals could enhance electron flow [167,168]. According to this approach, the higher catalytic activity of copper cobaltite catalysts with inverse spinel structures could also be explained by the enrichment of divalent Co and Cu cations in octahedral coordination, which could promote electron flow in redox reactions. Li et al. [169] prepared a series of Cu_xMn_y/TiO_2 catalysts for the purification of n-hexanal by adjusting the Cu loading and the Cu-Mn atomic ratio. The $Cu_{15}Mn_{15}/TiO_2$ catalyst performed the best activity, and the temperature with 90% conversion was 225 °C. It indicated that the copper-manganese spinel ($Cu_{1.5}Mn_{1.5}O_4$) with the strong interaction between Mn^{2+} and Cu^{2+} would generate a large number of oxygen vacancies and lattice defects, which provide a transfer channel for active species to promote the reaction together with the reactive oxygen species produced. The possible redox reaction of the $Cu_{1.5}Mn_{1.5}O_4$ component was: $Cu^{2+}+Mn^{2+}+Mn^{4+} \rightleftharpoons Mn^{3+}+Cu^+$, and the catalytic reaction mechanism is shown in Figure 8. As the surface-adsorbed oxygen oxidizes n-hexanal and consumes it continuously, the lattice oxygen was supplemented to generate oxygen vacancies. The gas phase oxygen oxidized the reduced catalyst to fill the oxygen vacancies, keeping the spinel structure stable while forming a

redox reaction cycle. Behar et al. [170] also found an excellent performance of $Cu_{1.5}Mn_{1.5}O_4$ catalyst in their experiment due to the complete conversion temperature of toluene being 240 °C. A similar redox reaction of the interaction between Cu and Mn ($Cu^{2+}+Mn^{3+} \leftrightarrow Mn^{4+}+Cu^+$) was proposed.
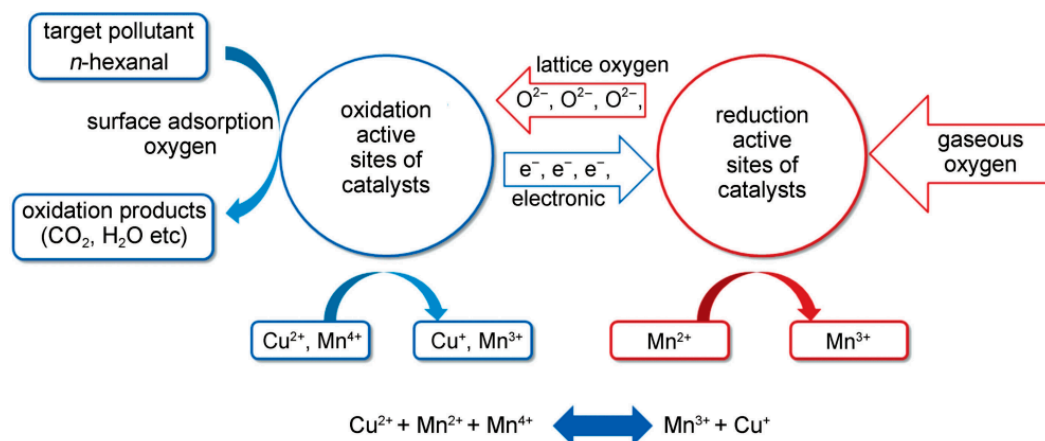

Figure 8. Oxidation-reduction mechanism of n-hexanal over Cu_xMn_y/TiO_2 catalyst [169].

Other composite catalysts

The composite oxide catalysts of $Mn-CeO_x/TiO_2/cordierite$ were prepared in the ultrasonic process and tested for their performance in the purification of NMHC to evaluate the purification effect of overall cooking oil fume [171]. Results showed the purification efficiency of NMHC could reach 93.6% at 400 °C. The reason is that ultrasonication would increase the specific surface area of the catalyst and thus improve the dispersion of active components. Besides, the interaction between Mn and Ce and the high ratios of Mn^{4+}/Mn^{3+}, Ce^{4+}/Ce^{3+} were beneficial in generating more reactive oxygen species and promoting the oxidization of NMHC. The catalytic performance of Cu-Co composite oxides with different ratios was also investigated [172]. The Cu_1Co_4 could remove 90% n-heptane at 186 °C. The morphologies of catalysts are shown in Figure 9. Compared with other catalysts, smaller and more uniform metal particles and porous structures were observed on the Cu_1Co_4 catalyst. These could increase the contact area between the catalyst and the reactants. The TPD characterization indicated that the oxygen desorption peak of Cu_1Co_4 was significantly enhanced due to the partial replacement of Co^{2+} in the spinel tetrahedral sites by Cu^{2+} and the increase of Co^{3+} in the octahedral sites, thus changing the coordination environment of oxygen species. The mobility of oxygen plays a vital role in catalytic performance. Furthermore, the addition of Cu significantly improved stability. The activity of the referenced Cu_0Co_5 catalyst decreased continuously during the reaction time, with n-heptane conversion decreasing from the initial 92% to 40% after 400 min. In contrast, the Cu_1Co_4 catalyst was stable under the same conditions, and the n-heptane conversion was basically maintained at 99% within 480 min without carbon deactivation. The catalytic performance and stability of composite metal catalysts were significantly improved compared with single metal catalysts.
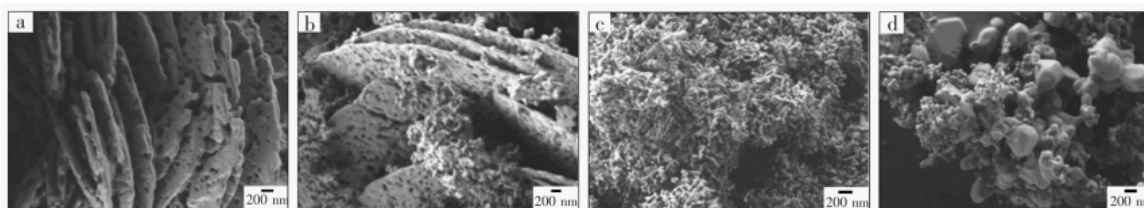

Figure 9. SEM of Cu/Co catalysts with different ratios: (**a**) Cu_0Cu_5; (**b**) Cu_1Co_8; (**c**) Cu_1Co_4; (**d**) Cu_1Co_2 [172].

Table 6. Non-noble metal oxide catalysts for catalytic oxidation of VOCs.

	Catalyst	Preparation	VOC	Concentration (ppm)	Space velocity (h^{-1})	Temp (°C)	Conversion (%)	References
Single metal catalysts	Co_3O_4	External template	Ethyl acetate	466.7	53,050	245	100	[149]
	CeO_2	Impregnation	Acetone	1000	15,000	250	85	[150]
	Mn/cordierite	Impregnation	Oil fume	5000	—	400	87.8	[151]
Perovskite catalysts	La_2CoMnO_6	Citrate	Toluene	300	30,000	300	100	[152]
	$LaMn_{0.25}Co_{0.75}O_3$	Sol-gel combustion	Propanol	—	5000	300	96	[153]
	$LaMnO_3$	Citrate sol–gel (SG)	Toluene	1000	15,000	225	100	[154]
	$La_{0.8}Sr_{0.2}MnO_{3+x}$	citric acid sol–gel	Ethyl acetate	500	20,000	159	99	[157]
	$La_{0.9}K_{0.1}MnO_3$	Citrate	Methyl ethyl ketone	1250	425	267	100	[158]
Spinel catalysts	$Co_xMn_{3-x}O_4$	Simple Synthesis	Toluene	1000	15,000	250	90	[160]
	$CuCo_2O_4$	Solvothermal	Acetone	1000	93,000	200	100	[161]
	$CuMn_2O_4$	Hard template	Toluene	1000	20,000	205	90	[162]
	$CuCo_2O_4/CeO_2$	Gel-burn	n-hexane	500	30,000	280	100	[166]
	$Cu_{1.5}Mn_{1.5}O_4$	Impregnation	Toluene	1000	—	240	100	[170]
Other composite catalysts	Cu_xMn_y/TiO_2	Coprecipitation	n-hexanal	—	25,000	225	90	[169]
	$Mn-CeO_x/TiO_2$	Sol-gel	NHMC	1500	—	400	93.6	[171]
	$Cu_1Co_4O_x$	Coprecipitation	n-heptane	—	15,000	186	90	[172]

5. Conclusions

VOCs in cooking oil fumes have been proven to be harmful to the environment and humans and urgently need to be removed. The components of cooking oil fume are complex, including hydrocarbons, ketone aldehydes, alcohol ethers, acid esters, polycyclic compounds, and other species. The emission characteristics of cooking fumes are influenced by the type of oil, temperature, and cuisine. In general, the oil with more unsaturated fatty acids releases higher concentrations of VOCs. As the cooking temperature increases, the concentration of VOCs significantly increases. At relatively low temperatures (under 200 °C), the composition of VOCs mainly contains aliphatic hydrocarbons, ketones, and aldehydes. Increasing to above 250 °C increased the contents of aromatic hydrocarbons and acid esters. The emission concentrations in grilled cuisine are significantly higher than in non-grilled cuisines. The former is mainly composed of hydrocarbons, while the latter mainly consists of alkanes, alcohols, and aldehydes. Overall, the VOC problem for Chinese cuisine is more serious due to the various cooking styles, which need more attention to purify cooking oil fume pollutants.

Various purification methods of cooking oil fume, including physical capture, chemical decomposition, and combination methods, are compared. The physical capture methods mainly focus on the removal of particulate matter, while the chemical decomposition methods mainly decompose VOCs into small molecules such as CO_2 and H_2O. Although the chemical decomposition methods are more expensive than the physical capture methods, they are more efficient in the overall removal of cooking oil fume pollutants without secondary pollution. Furthermore, combining the two types of methods to form combination purification methods can effectively remove particulate matter as well as VOCs. The catalytic combustion method can effectively remove VOCs without causing secondary pollution, which has a broad application prospect. Commonly used catalysts include noble metal and non-noble metal catalysts. Noble metal catalysts (Au, Pt, and Pd) can completely oxidize VOCs below 300 °C, but they are expensive and easily deactivated due to agglomeration and sintering at higher temperatures. Suitable carriers and additives are beneficial to improve the catalytic activity and reduce the cost. In order to improve the economy, transition metals (Cu, Mn, Ce, etc.) in non-noble metals are worth considering. They have good catalytic properties due to their different valence states and strong electron transfer ability. Non-noble metal catalysts can be mainly divided into single metal and

composite metal catalysts, while the composite metal catalysts include perovskite, spinel, and other composite catalysts. They have great potential for application with high activity and a good economy.

Although studies have shown that catalytic combustion is an effective method to remove VOCs in cooking oil fumes, there are still many problems that need to be solved to promote its practical application. (1) Most of the current studies have mainly focused on single-component model compounds. The actual cooking oil fume contains multiple components, and the components may interact with each other, which requires in-depth research. (2) The actual cooking oil fume usually contains water. It is a challenge to develop catalysts with high efficiency and strong water resistance. (3) The composition and concentration of VOCs in cooking oil fume are significantly influenced by temperature. In order to meet the removal demand of VOCs at different temperatures, a combination of condition-adaptive technologies can be considered. (4) The degradation efficiency of VOCs needs to be improved. To further purify the VOCs, future work would focus on new catalysts with high activity and stability at low temperatures. Besides, multi-field synergistic technologies exist, such as photo-thermal catalysis and electro-thermal catalysis.

Author Contributions: Conceptualization, C.T. and L.H.; investigation, X.Z., H.L. and Q.R.; writing—original draft preparation, C.T. and L.H.; writing—review and editing, C.T., L.H. and S.H.; supervision, S.S., Y.W., S.H. and J.X.; funding acquisition, Y.W. and H.H. All authors have read and agreed to the published version of the manuscript.

Data Availability Statement: Not applicable.

Conflicts of Interest: The authors declare no conflict of interest.

References

1. Chen, T.Y.; Fang, Y.H.; Chen, H.L.; Chang, C.H.; Huang, H.; Chen, Y.S.; Liao, K.M.; Wu, H.Y.; Chang, G.C.; Tsai, Y.H.; et al. Impact of cooking oil fume exposure and fume extractor use on lung cancer risk in non-smoking Han Chinese women. *Sci. Rep.* **2020**, *10*, 6774. [CrossRef] [PubMed]
2. Hung, H.S.; Wu, W.J.; Cheng, Y.W.; Wu, T.C.; Chang, K.L.; Lee, H. Association of cooking oil fumes exposure with lung cancer: Involvement of inhibitor of apoptosis proteins in cell survival and proliferation in vitro. *Mutat. Res. Genet. Toxicol. Environ. Mutagen.* **2007**, *628*, 107–116. [CrossRef] [PubMed]
3. Chang, S.S.; Peterson, R.J.; Ho, C.T. Chemical reactions involved in the deep-fat frying of foods1. *J. Am. Oil Chem. Soc.* **1978**, *55*, 718–727. [CrossRef] [PubMed]
4. He, Z.; Wang, X.; Ling, Z.; Zhao, J.; Guo, H.; Shao, M.; Wang, Z. Contributions of different anthropogenic volatile organic compound sources to ozone formation at a receptor site in the Pearl River Delta region and its policy implications. *Atmos. Chem. Phys.* **2019**, *19*, 8801–8816. [CrossRef]
5. Yin, Z.; Li, H.; Cui, Z.; Ren, Y.; Li, X.; Wu, W.; Guan, P.; Qian, B.; Rothman, N.; Lan, Q.; et al. Polymorphisms in pre-miRNA genes and cooking oil fume exposure as well as their interaction on the risk of lung cancer in a Chinese nonsmoking female population. *OncoTargets Ther.* **2016**, *9*, 395–401. [CrossRef]
6. Huang, B.; Lei, C.; Wei, C.; Zeng, G. Chlorinated volatile organic compounds (Cl-VOCs) in environment—Sources, potential human health impacts, and current remediation technologies. *Environ. Int.* **2014**, *71*, 118–138. [CrossRef]
7. Huang, Y.; Ho, S.S.H.; Ho, K.F.; Lee, S.C.; Yu, J.Z.; Louie, P.K.K. Characteristics and health impacts of VOCs and carbonyls associated with residential cooking activities in Hong Kong. *J. Hazard. Mater.* **2011**, *186*, 344–351. [CrossRef]
8. Song, S.K.; Shon, Z.H.; Kang, Y.H.; Kim, K.H.; Han, S.B.; Kang, M.; Bang, J.H.; Oh, I. Source apportionment of VOCs and their impact on air quality and health in the megacity of Seoul. *Environ. Pollut.* **2019**, *247*, 763–774. [CrossRef]
9. Kampa, M.; Castanas, E. Human health effects of air pollution. *Environ. Pollut.* **2008**, *151*, 362–367. [CrossRef]
10. Pöschl, U. Atmospheric aerosols: Composition, transformation, climate and health effects. *Angew. Chem. Int. Ed.* **2005**, *44*, 7520–7540. [CrossRef]
11. Mauderly, J.L.; Chow, J.C. Health effects of organic aerosols. *Inhal. Toxicol.* **2008**, *20*, 257–288. [CrossRef] [PubMed]
12. Billionnet, C.; Sherrill, D.; Annesi-Maesano, I. Estimating the health effects of exposure to multi-pollutant mixture. *Ann. Epidemiol.* **2012**, *22*, 126–141. [CrossRef] [PubMed]

13. Mitchell, C.S.; Zhang, J.; Sigsgaard, T.; Jantunen, M.; Lioy, P.J.; Samson, R.; Karol, M.H. Current state of the science: Health effects and indoor environmental quality. *Environ. Health Perspect.* **2007**, *115*, 958–964. [CrossRef]

14. Ahmed, F.E. Toxicology and human health effects following exposure to oxygenated or reformulated gasoline. *Toxicol. Lett.* **2001**, *123*, 89–113. [CrossRef] [PubMed]

15. Pathak, A.K.; Swargiary, K.; Kongsawang, N.; Jitpratak, P.; Ajchareeyasoontorn, N.; Udomkittivorakul, J.; Viphavakit, C. Recent Advances in Sensing Materials Targeting Clinical Volatile Organic Compound (VOC) Biomarkers: A Review. *Biosensors* **2023**, *13*, 114. [CrossRef]

16. Zhao, Q.; Li, Y.; Chai, X.; Xu, L.; Zhang, L.; Ning, P.; Huang, J.; Tian, S. Interaction of inhalable volatile organic compounds and pulmonary surfactant: Potential hazards of VOCs exposure to lung. *J. Hazard. Mater.* **2019**, *369*, 512–520. [CrossRef]

17. Fiedler, N.; Laumbach, R.; Kelly-McNeil, K.; Lioy, P.; Fan, Z.H.; Zhang, J.; Ottenweller, J.; Ohman-Strickland, P.; Kipen, H. Health effects of a mixture of indoor air volatile organics, their ozone oxidation products, and stress. *Environ. Health Perspect.* **2005**, *113*, 1542–1548. [CrossRef]

18. Peng, C.Y.; Lan, C.H.; Lin, P.C.; Kuo, Y.C. Effects of cooking method, cooking oil, and food type on aldehyde emissions in cooking oil fumes. *J. Hazard. Mater.* **2017**, *324*, 160–167. [CrossRef]

19. Li, M.; Yin, Z.; Guan, P.; Li, X.; Cui, Z.; Zhang, J.; Bai, W.; He, Q.; Zhou, B. XRCC1 polymorphisms, cooking oil fume and lung cancer in Chinese women nonsmokers. *Lung Cancer* **2008**, *62*, 145–151. [CrossRef]

20. Biró, A.; Pállinger, É.; Major, J.; Jakab, M.G.; Klupp, T.; Falus, A.; Tompa, A. Lymphocyte phenotype analysis and chromosome aberration frequency of workers occupationally exposed to styrene, benzene, polycyclic aromatic hydrocarbons or mixed solvents. *Immunol. Lett.* **2002**, *81*, 133–140. [CrossRef]

21. Rao, R.; Ma, S.; Gao, B.; Bi, F.; Chen, Y.; Yang, Y.; Liu, N.; Wu, M.; Zhang, X. Recent advances of metal-organic framework-based and derivative materials in the heterogeneous catalytic removal of volatile organic compounds. *J. Colloid Interface Sci.* **2023**, *636*, 55–72. [CrossRef]

22. Zhang, J.; Xu, X.; Zhao, S.; Meng, X.; Xiao, F.S. Recent advances of zeolites in catalytic oxidations of volatile organic compounds. *Catal. Today* **2023**, *410*, 56–67. [CrossRef]

23. Goicoechea, E.; Guillén, M.D. Volatile compounds generated in corn oil stored at room temperature. Presence of toxic compounds. *Eur. J. Lipid Sci. Technol.* **2014**, *116*, 395–406. [CrossRef]

24. Hosseini, H.; Ghorbani, M.; Meshginfar, N.; Mahoonak, A.S. A review on frying: Procedure, fat, deterioration progress and health hazards. *J. Am. Oil Chem. Soc.* **2016**, *93*, 445–466. [CrossRef]

25. Juárez, M.D.; Osawa, C.C.; Acuña, M.E.; Sammán, N.; Gonçalves, L.A.G. Degradation in soybean oil, sunflower oil and partially hydrogenated fats after food frying, monitored by conventional and unconventional methods. *Food Control* **2011**, *22*, 1920–1927. [CrossRef]

26. Kabir, E.; Kim, K.H. An investigation on hazardous and odorous pollutant emission during cooking activities. *J. Hazard. Mater.* **2011**, *188*, 443–454. [CrossRef] [PubMed]

27. Lin, Y.; Shao, M.; Lu, S. The emission characteristics of hydrocarbon from Chinese cooking under smoke control. *Int. J. Environ. Anal. Chem.* **2010**, *90*, 708–721. [CrossRef]

28. Schauer, J.J.; Kleeman, M.J.; Cass, G.R.; Simoneit, B.R.T. Measurement of emissions from air pollution sources. 4. C1−C27 organic compounds from cooking with seed oils. *Environ. Sci. Technol.* **2002**, *36*, 567–575. [CrossRef]

29. Molina-Garcia, L.; Santos, C.S.P.; Cunha, S.C.; Casal, S.; Fernandes, J.O. Comparative fingerprint changes of toxic volatiles in low PUFA vegetable oils under deep-frying. *J. Am. Oil Chem. Soc.* **2017**, *94*, 271–284. [CrossRef]

30. Klein, F.; Platt, S.M.; Farren, N.J.; Detournay, A.; Bruns, E.A.; Bozzetti, C.; Daellenbach, K.R.; Kilic, D.; Kumar, N.K.; Pieber, S.M.; et al. Characterization of gas-phase organics using proton transfer reaction time-of-flight mass spectrometry: Cooking emissions. *Environ. Sci. Technol.* **2016**, *50*, 1243–1250. [CrossRef]

31. Zhang, D.C.; Liu, J.J.; Jia, L.Z.; Wang, P.; Han, X. Speciation of VOCs in the cooking fumes from five edible oils and their corresponding health risk assessments. *Atmos. Environ.* **2019**, *211*, 6–17. [CrossRef]

32. Guillen, M.D.; Goicoechea, E. Formation of oxygenated α, β-unsaturated aldehydes and other toxic compounds in sunflower oil oxidation at room temperature in closed receptacles. *Food Chem.* **2008**, *111*, 157–164. [CrossRef]

33. Chen, Y.; Yang, Y.; Nie, S.; Yang, X.; Wang, Y.; Yang, M.; Li, C.; Xie, M. The analysis of trans fatty acid profiles in deep frying palm oil and chicken fillets with an improved gas chromatography method. *Food Control* **2014**, *44*, 191–197. [CrossRef]

34. He, W.; Nie, L.; Tian, G.; Li, J.; Shao, X.; Wang, M.Y. Study on the chemical compositions of VOCs emitted by cooking oils based on GC-MS. *Environ. Sci.* **2013**, *34*, 4605–4611.

35. Lin, J.S.; Chuang, K.T.; Huang, M.S.; Wei, K.M. Emission of ethylene oxide during frying of foods in soybean oil. *Food Chem. Toxicol.* **2007**, *45*, 568–574. [CrossRef]

36. Cheng, S.; Wang, G.; Lang, J.; Wen, W.; Wang, X.; Yao, S. Characterization of volatile organic compounds from different cooking emissions. *Atmos. Environ.* **2016**, *145*, 299–307. [CrossRef]

37. He, W.; Shi, A.; Shao, X.; Nie, L.; Wang, T.; Li, G. Insights into the comprehensive characteristics of volatile organic compounds from multiple cooking emissions and aftertreatment control technologies application. *Atmos. Environ.* **2020**, *240*, 117646. [CrossRef]

38. Cui, T.; Cheng, J.; He, W.; Ren, P.; Nie, L.; Xu, D.; Pan, T. Emission Characteristics of VOCs from Typical Restaurants in Beijing. *Environ. Sci.* **2015**, *36*, 1523–1529.

39. Zhang, H.; Yang, H.; Wang, S.; Zhang, Y.; Li, D.; Zhang, X. Research progress on purification technology for catering oil fume pollutants. *Mod. Chem. Ind.* **2020**, *40*, 71–75.

40. Wang, L.; Xiang, Z.; Stevanovic, S.; Ristovski, Z.; Salimi, F.; Gao, J.; Wang, H.; Li, L. Role of Chinese cooking emissions on ambient air quality and human health. *Sci. Total Environ.* **2017**, *589*, 173–181. [CrossRef]

41. Zhao, Y.; Zhao, B. Emissions of air pollutants from Chinese cooking: A literature review. In *Building Simulation*; Springer: Berlin/Heidelberg, Germany, 2018; Volume 11, pp. 977–995.

42. Yan, R.; Li, M.; Wang, Y.; Fu, Y. Analysis for Improvement of Kitchen Odour by Oil Fume Purification Technology. *Chem. Eng. Trans.* **2018**, *68*, 415–420.

43. Zhao, Q.C.; Chen, C.; Zhang, J.T.; Hu, P.J.; Zhang, X.J. Performance of Cooking Aerosol Treatment in China Catering: A Review and Assessment. *Pol. J. Environ. Stud.* **2021**, *30*, 1923–1933. [CrossRef]

44. Karagoz, I.; Avci, A.; Surmen, A.; Sendogan, O. Design and performance evaluation of a new cyclone separator. *J. Aerosol Sci.* **2013**, *59*, 57–64. [CrossRef]

45. Hou, J.Q.; Li, M.X.; Wei, Z.M.; Xi, B.D.; Jia, X.; Zhu, C.W.; Liu, D.M. Critical components of odors and VOCs in mechanical biological treatment process of MSW. In *Advanced Materials Research*; Trans Tech Publications Ltd.: Wollerau, Switzerland, 2013; Volume 647, pp. 438–449.

46. An, T.; Huang, Y.; Li, G.; He, Z.; Chen, J.; Zhang, C. Pollution profiles and health risk assessment of VOCs emitted during e-waste dismantling processes associated with different dismantling methods. *Environ. Int.* **2014**, *73*, 186–194. [CrossRef] [PubMed]

47. Wallner, P.; Munoz, U.; Tappler, P.; Wanka, A.; Kundi, M.; Shelton, J.F.; Hutter, H.P. Indoor environmental quality in mechanically ventilated, energy-efficient buildings vs. conventional buildings. *Int. J. Environ. Res. Public Health* **2015**, *12*, 14132–14147. [CrossRef]

48. Hyttinen, M.; Pasanen, P.; Kalliokoski, P. Adsorption and desorption of selected VOCs in dust collected on air filters. *Atmos. Environ.* **2001**, *35*, 5709–5716. [CrossRef]

49. Kim, K.J.; Kang, C.S.; You, Y.J.; Chung, M.C.; Woo, M.W.; Jeong, W.J.; Park, N.C.; Ahn, H.G. Adsorption–desorption characteristics of VOCs over impregnated activated carbons. *Catal. Today* **2006**, *111*, 223–228. [CrossRef]

50. Gallego, E.; Roca, F.J.; Perales, J.F.; Guardino, X. Experimental evaluation of VOC removal efficiency of a coconut shell activated carbon filter for indoor air quality enhancement. *Build. Environ.* **2013**, *67*, 14–25. [CrossRef]

51. Kadam, V.; Truong, Y.B.; Easton, C.; Mukherjee, S.; Wang, L.; Padhye, R.; Kyratzis, L. Electrospun polyacrylonitrile/β-cyclodextrin composite membranes for simultaneous air filtration and adsorption of volatile organic compounds. *ACS Appl. Nano Mater.* **2018**, *1*, 4268–4277. [CrossRef]

52. Lalanne, F.; Malhautier, L.; Roux, J.C.; Fanlo, J.L. Absorption of a mixture of volatile organic compounds (VOCs) in aqueous solutions of soluble cutting oil. *Bioresour. Technol.* **2008**, *99*, 1699–1707. [CrossRef]

53. Heymes, F.; Demoustier, P.M.; Charbit, F.; Fanlo, J.L.; Moulin, P. Treatment of gas containing hydrophobic VOCs by a hybrid absorption–pervaporation process: The case of toluene. *Chem. Eng. Sci.* **2007**, *62*, 2576–2589. [CrossRef]

54. Tamaddoni, M.; Sotudeh-Gharebagh, R.; Nario, S.; Hajihosseinzadeh, M.; Mostoufi, N. Experimental study of the VOC emitted from crude oil tankers. *Process Saf. Environ. Prot.* **2014**, *92*, 929–937. [CrossRef]

55. Quijano, G.; Couvert, A.; Amrane, A.; Darracq, G.; Couriol, C.; Cloirec, P.L.; Paquin, L.; Carrié, D. Potential of ionic liquids for VOC absorption and biodegradation in multiphase systems. *Chem. Eng. Sci.* **2011**, *66*, 2707–2712. [CrossRef]

56. Hoenig, S.A. New applications of electrostatic technology to control of dust, fumes, smokes, and aerosols. *IEEE Trans. Ind. Appl.* **1981**, *IA-17*, 386–391. [CrossRef]

57. Cheng, J.; Liu, J.; Wang, T.; Sui, Z.; Zhang, Y.; Pan, W.P. Reductions in volatile organic compound emissions from coal-fired power plants by combining air pollution control devices and modified fly ash. *Energy Fuels* **2019**, *33*, 2926–2933. [CrossRef]

58. Shirsat, M.D.; Sarkar, T.; Kakoullis, J., Jr.; Myung, N.V.; Konnanath, B.; Spanias, A.; Mulchandani, A. Porphyrin-functionalized single-walled carbon nanotube chemiresistive sensor arrays for VOCs. *J. Phys. Chem. C* **2012**, *116*, 3845–3850. [CrossRef]

59. Benjamin, O.; Silcock, P.; Beauchamp, J.; Buettner, A.; Everett, D.W. Volatile release and structural stability of β-lactoglobulin primary and multilayer emulsions under simulated oral conditions. *Food Chem.* **2013**, *140*, 124–134. [CrossRef]

60. Dziembaj, R.; Molenda, M.; Chmielarz, L.; Drozdek, M.; Zaitz, M.M.; Dudek, B.; Rafalska-Łasocha, A.; Piwowarska, Z. Nanostructured Cu-doped ceria obtained by reverse microemulsion method as catalysts for incineration of selected VOCs. *Catal. Lett.* **2010**, *135*, 68–75. [CrossRef]

61. Zagoruiko, A.N.; Kostenko, O.V.; Noskov, A.S. Development of the adsorption-catalytic reverse-process for incineration of volatile organic compounds in diluted waste gases. *Chem. Eng. Sci.* **1996**, *51*, 2989–2994. [CrossRef]

62. Schwärzle, A.; Monz, T.O.; Aigner, M. Thermal Incineration of VOCs in a Jet-Stabilized Micro Gas Turbine Combustor. In Proceedings of the Turbo Expo: Power for Land, Sea, and Air, Montreal, QC, Canada, 15–19 June 2015. [CrossRef]

63. Van der Vaart, D.R.; Vatvuk, W.M.; Wehe, A.H. Thermal and catalytic incinerators for the control of VOCs. *J. Air Waste Manag. Assoc.* **1991**, *41*, 92–98. [CrossRef]

64. Huang, Y.H.; Yi, H.H.; Tang, X.L.; Zhao, S.Z.; Feng, T.C. Research progress in the removal of cooking oil fumes by catalytic combustion. *Chem. Ind. Eng. Prog.* **2017**, *36*, 1270–1277.

65. Li, W.B.; Wang, J.X.; Gong, H. Catalytic combustion of VOCs on non-noble metal catalysts. *Catal. Today* **2009**, *148*, 81–87. [CrossRef]

66. Kim, S.C.; Shim, W.G. Catalytic combustion of VOCs over a series of manganese oxide catalysts. *Appl. Catal. B Environ.* **2010**, *98*, 180–185. [CrossRef]

67. Aguero, F.N.; Barbero, B.P.; Gambaro, L.; Cadu's, L.E. Catalytic combustion of volatile organic compounds in binary mixtures over MnO_x/Al_2O_3 catalyst. *Appl. Catal. B Environ.* **2009**, *91*, 108–112. [CrossRef]

68. Tian, Z.Y.; Ngamou, P.H.T.; Vannier, V.; Kohse-Höinghaus, K.; Bahlawane, N. Catalytic oxidation of VOCs over mixed Co–Mn oxides. *Appl. Catal. B Environ.* **2012**, *117*, 125–134. [CrossRef]

69. Chang, Z.; Wang, C.; Zhang, G. Progress in degradation of volatile organic compounds based on low-temperature plasma technology. *Plasma Process. Polym.* **2020**, *17*, 1900131. [CrossRef]

70. Fenglei, H.; Mengyu, L.; Huangrong, Z.; Ting, L.; Dandan, L.; Shuo, Z.; Wenwen, G.; Fang, L. Product analysis and mechanism of toluene degradation by low temperature plasma with single dielectric barrier discharge. *J. Saudi Chem. Soc.* **2020**, *24*, 673–682. [CrossRef]

71. Zhang, Z.; Jiang, Z.; Shangguan, W. Low-temperature catalysis for VOCs removal in technology and application: A state-of-the-art review. *Catal. Today* **2016**, *264*, 270–278. [CrossRef]

72. Aerts, R.; Tu, X.; De Bie, C.; Whitehead, J.C.; Bogaerts, A. An investigation into the dominant reactions for ethylene destruction in non-thermal atmospheric plasmas. *Plasma Process. Polym.* **2012**, *9*, 994–1000. [CrossRef]

73. Xiao, G.; Xu, W.; Wu, R.; Ni, M.; Du, C.; Gao, X.; Luo, Z.; Cen, K. Non-thermal plasmas for VOCs abatement. *Plasma Chem. Plasma Process.* **2014**, *34*, 1033–1065. [CrossRef]

74. Kang, I.S.; Xi, J.; Hu, H.Y. Photolysis and photooxidation of typical gaseous VOCs by UV Irradiation: Removal performance and mechanisms. *Front. Environ. Sci. Eng.* **2018**, *12*, 1–14. [CrossRef]

75. Huang, H.; Huang, H.; Zhan, Y.; Liu, G.; Wang, X.; Lu, H.; Xiao, L.; Feng, Q.; Leung DY, C. Efficient degradation of gaseous benzene by VUV photolysis combined with ozone-assisted catalytic oxidation: Performance and mechanism. *Appl. Catal. B Environ.* **2016**, *186*, 62–68. [CrossRef]

76. Xie, R.; Lei, D.; Xie, X.; Suo, Z.; Leung DY, C.; Cao, J.; Ruimei, F.; Huang, H. Accelerated oxidation of VOCs via vacuum ultraviolet photolysis coupled with wet scrubbing process. *J. Environ. Sci.* **2022**. [CrossRef]

77. Shayegan, Z.; Haghighat, F.; Lee, C.S. Photocatalytic oxidation of volatile organic compounds for indoor environment applications: Three different scaled setups. *Chem. Eng. J.* **2019**, *357*, 533–546. [CrossRef]

78. Ji, J.; Xu, Y.; Huang, H.; He, M.; Liu, S.; Liu, G.; Xie, R.; Feng, Q.; Shu, Y.; Zhan, Y.; et al. Mesoporous TiO_2 under VUV irradiation: Enhanced photocatalytic oxidation for VOCs degradation at room temperature. *Chem. Eng. J.* **2017**, *327*, 490–499. [CrossRef]

79. Yoshikawa, M.; Zhang, M.; Toyota, K. Biodegradation of volatile organic compounds and their effects on biodegradability under co-existing conditions. *Microbes Environ.* **2017**, *32*, 188–200. [CrossRef] [PubMed]

80. Estrada, J.M.; Rodríguez, E.; Quijano, G.; Muñoz, R. Influence of gaseous VOC concentration on the diversity and biodegradation performance of microbial communities. *Bioprocess Biosyst. Eng.* **2012**, *35*, 1477–1488. [CrossRef]

81. Yang, C.; Qian, H.; Li, X.; Cheng, Y.; He, H.; Zeng, G.; Xi, J. Simultaneous removal of multicomponent VOCs in biofilters. *Trends Biotechnol.* **2018**, *36*, 673–685. [CrossRef]

82. Estrada, J.M.; Hernández, S.; Muñoz, R.; Revah, S. A comparative study of fungal and bacterial biofiltration treating a VOC mixture. *J. Hazard. Mater.* **2013**, *250*, 190–197. [CrossRef]

83. Qu, M.; Cheng, Z.; Sun, Z.; Chen, D.; Yu, J.; Chen, J. Non-thermal plasma coupled with catalysis for VOCs abatement: A review. *Process Saf. Environ. Prot.* **2021**, *153*, 139–158. [CrossRef]

84. Jeon, E.C.; Kim, K.J.; Kim, J.C.; Kim, K.H.; Chung, S.G.; Sunwoo, Y.; Park, Y.K. Novel hybrid technology for VOC control using an electron beam and catalyst. *Res. Chem. Intermed.* **2008**, *34*, 863–870. [CrossRef]

85. Aouadi, I.; Tatibouët, J.M.; Bergaoui, L. MnO_x/TiO_2 catalysts for VOCs abatement by coupling non-thermal plasma and photocatalysis. *Plasma Chem. Plasma Process.* **2016**, *36*, 1485–1499. [CrossRef]

86. Xie, R.; Ji, J.; Guo, K.; Lei, D.; Fan, Q.; Leung, D.Y.C.; Huang, H. Wet scrubber coupled with UV/PMS process for efficient removal of gaseous VOCs: Roles of sulfate and hydroxyl radicals. *Chem. Eng. J.* **2019**, *356*, 632–640. [CrossRef]

87. Aziz, A.; Kim, K.S. Synergistic effect of UV pretreated Fe-ZSM-5 catalysts for heterogeneous catalytic complete oxidation of VOC: A technology development for sustainable use. *J. Hazard. Mater.* **2017**, *340*, 351–359. [CrossRef]

88. Oliva, G.; Comia, J.R.; Senatore, V.; Zarra, T.; Ballestreros, F.; Belgiorno, V.; Naddeo, V. Degradation of gaseous volatile organic compounds (VOCs) by a novel UV-ozone technology. *Sci. Rep.* **2022**, *12*, 11112. [CrossRef]

89. Darracq, G.; Couvert, A.; Couriol, C.; Amrane, A.; Cloirec, P.L. Removal of hydrophobic volatile organic compounds in an integrated process coupling absorption and biodegradation—Selection of an organic liquid phase. *Water Air Soil Pollut.* **2012**, *223*, 4969–4997. [CrossRef]

90. Moussavi, G.; Mohseni, M. Using UV pretreatment to enhance biofiltration of mixtures of aromatic VOCs. *J. Hazard. Mater.* **2007**, *144*, 59–66. [CrossRef]

91. Feng, X.; Liu, H.; He, C.; Shen, Z.; Wang, T. Synergistic effects and mechanism of a non-thermal plasma catalysis system in volatile organic compound removal: A review. *Catal. Sci. Technol.* **2018**, *8*, 936–954. [CrossRef]

92. Mohseni, M.; Zhao, J.L. Coupling ultraviolet photolysis and biofiltration for enhanced degradation of aromatic air pollutants. *J. Chem. Technol. Biotechnol. Int. Res. Process Environ. Clean Technol.* **2006**, *81*, 146–151. [CrossRef]

93. Chen, J.; Huang, Y.; Li, G.; An, T.; Hu, Y.; Li, Y. VOCs elimination and health risk reduction in e-waste dismantling workshop using integrated techniques of electrostatic precipitation with advanced oxidation technologies. *J. Hazard. Mater.* **2016**, *302*, 395–403. [CrossRef]

94. Maciuca, A.; Batiot-Dupeyrat, C.; Tatibouët, J.M. Synergetic effect by coupling photocatalysis with plasma for low VOCs concentration removal from air. *Appl. Catal. B Environ.* **2012**, *125*, 432–438. [CrossRef]

95. He, Z.; Li, J.; Chen, J.; Chen, Z.; Li, G.; Sun, G.; An, T. Treatment of organic waste gas in a paint plant by combined technique of biotrickling filtration with photocatalytic oxidation. *Chem. Eng. J.* **2012**, *200*, 645–653. [CrossRef]

96. Kamal, M.S.; Razzak, S.A.; Hossain, M.M. Catalytic oxidation of volatile organic compounds (VOCs)-A review. *Atmos. Environ.* **2016**, *140*, 117–134. [CrossRef]

97. Specchia, S.; Conti, F.; Specchia, V. Kinetic Studies on $Pd/Ce_xZr_{1-x}O_2$ Catalyst for Methane Combustion. *Ind. Eng. Chem. Res.* **2010**, *49*, 11101–11111. [CrossRef]

98. Zhang, K.; Ding, H.; Pan, W.; Mu, X.; Qiu, K.; Ma, J.; Zhao, Y.; Song, J.; Zhang, Z. Research progress of a composite metal oxide catalyst for VOC degradation. *Environ. Sci. Technol.* **2022**, *56*, 9220–9236. [CrossRef]

99. Minicò, S.; Scirè, S.; Crisafulli, C.; Maggiore, R.; Galvagno, S. Catalytic combustion of volatile organic compounds on gold/iron oxide catalysts. *Appl. Catal. B Environ.* **2000**, *28*, 245–251. [CrossRef]

100. Tseng, T.K.; Chu, H. The kinetics of catalytic incineration of styrene over a MnO/Fe_2O_3 catalyst. *Sci. Total Environ.* **2001**, *275*, 83–93. [CrossRef]

101. Bedia, J.; Rosas, J.M.; Rodríguez-Mirasol, J.; Cordero, T. Pd supported on mesoporous activated carbons with high oxidation resistance as catalysts for toluene oxidation. *Appl. Catal. B Environ.* **2010**, *94*, 8–18. [CrossRef]

102. Spivey, J.J. Complete catalytic oxidation of volatile organics. *Ind. Eng. Chem. Res.* **1987**, *26*, 2165–2180. [CrossRef]

103. Zhu, L.; Shen, D.; Luo, K.H. A critical review on VOCs adsorption by different porous materials: Species, mechanisms and modification methods. *J. Hazard. Mater.* **2020**, *389*, 122102. [CrossRef]

104. Choudhary, V.R.; Deshmukh, G.M. Kinetics of the complete combustion of dilute propane and methyl ethyl ketone over Cr-doped ZrO_2 catalyst. *Chem. Eng. Sci.* **2005**, *60*, 1575–1581. [CrossRef]

105. Radic, N.; Grbic, B.; Terlecki-Baricevic, A. Kinetics of deep oxidation of n-hexane and toluene over Pt/Al_2O_3 catalysts: Platinum crystallite size effect. *Appl. Catal. B Environ.* **2004**, *50*, 153–159. [CrossRef]

106. Gatica, J.M.; Castiglioni, J.; de los Santos, C.; Yeste, M.P.; Cifredo, G.; Torres, M.; Vidal, H. Use of pillared clays in the preparation of washcoated clay honeycomb monoliths as support of manganese catalysts for the total oxidation of VOCs. *Catal. Today* **2017**, *296*, 84–94. [CrossRef]

107. Genty, E.; Siffert, S.; Cousin, R. Investigation of reaction mechanism and kinetic modelling for the toluene total oxidation in presence of CoAlCe catalyst. *Catal. Today* **2019**, *333*, 28–35. [CrossRef]

108. Hosseini, M.; Barakat, T.; Cousin, R.; Aboukaïs, A.; Su, B.L.; Weireld, G.D.; Siffert, S. Catalytic performance of core–shell and alloy Pd–Au nanoparticles for total oxidation of VOC: The effect of metal deposition. *Appl. Catal. B Environ.* **2012**, *111*, 218–224. [CrossRef]

109. Hu, C. Catalytic combustion kinetics of acetone and toluene over $Cu_{0.13}Ce_{0.87}Oy$ catalyst. *Chem. Eng. J.* **2011**, *168*, 1185–1192. [CrossRef]

110. Aranzabal, A.; Ayastuy-Arizti, J.L.; González-Marcos, J.A.; González-Velasco, J.R. The reaction pathway and kinetic mechanism of the catalytic oxidation of gaseous lean TCE on Pd/alumina catalysts. *J. Catal.* **2003**, *214*, 130–135. [CrossRef]

111. Banu, I.; Manta, C.M.; Bercaru, G.; Bozga, G. Combustion kinetics of cyclooctane and its binary mixture with o-xylene over a Pt/γ-alumina catalyst. *Chem. Eng. Res. Des.* **2015**, *102*, 399–406. [CrossRef]

112. Song, K.S.; Klvana, D.; Kirchnerova, J. Kinetics of propane combustion over $La_{0.66}Sr_{0.34}Ni_{0.3}Co_{0.7}O_3$ perovskite. *Appl. Catal. A Gen.* **2001**, *213*, 113–121. [CrossRef]

113. Li, T.Y.; Chiang, S.J.; Liaw, B.J.; Chen, Y.Z. Catalytic oxidation of benzene over $CuO/Ce_{1-x}Mn_xO_2$ catalysts. *Appl. Catal. B Environ.* **2011**, *103*, 143–148. [CrossRef]

114. Everaert, K.; Baeyens, J. Catalytic combustion of volatile organic compounds. *J. Hazard. Mater.* **2004**, *109*, 113–139. [CrossRef] [PubMed]

115. Behar, S.; Gómez-Mendoza, N.A.; Gómez-García, M.Á.; Šwierczyński, D.; Quignard, F.; Tanchoux, N. Study and modelling of kinetics of the oxidation of VOC catalyzed by nanosized Cu–Mn spinels prepared via an alginate route. *Appl. Catal. A Gen.* **2015**, *504*, 203–210. [CrossRef]

116. Burgos, N.; Paulis, M.; Antxustegi, M.M.; Montes, M. Deep oxidation of VOC mixtures with platinum supported on Al_2O_3/Al monoliths. *Appl. Catal. B Environ.* **2002**, *38*, 251–258. [CrossRef]

117. Lu, F.; Shen, B.; Li, S.; Liu, L.; Zhao, P.; Si, M. Exposure characteristics and risk assessment of VOCs from Chinese residential cooking. *J. Environ. Manag.* **2021**, *289*, 112535. [CrossRef]

118. Mizuno, N.; Kamata, K. Catalytic oxidation of hydrocarbons with hydrogen peroxide by vanadium-based polyoxometalates. *Coord. Chem. Rev.* **2011**, *255*, 2358–2370. [CrossRef]

119. Diehl, F.; Barbier, J., Jr.; Duprez, D.; Guibard, I.; Mabilon, G. Catalytic oxidation of heavy hydrocarbons over Pt/Al_2O_3. Influence of the structure of the molecule on its reactivity. *Appl. Catal. B Environ.* **2010**, *95*, 217–227. [CrossRef]

120. Diaz, C.C.; Yeste, M.P.; Vidal, H.; Gatica, J.M.; Cadús, L.E. In situ generation of $Mn_{1-x}Ce_x$ system on cordierite monolithic supports for combustion of n-hexane. Effects on activity and stability. *Fuel* **2020**, *262*, 116564. [CrossRef]

121. Ousmane, M.; Liotta, L.F.; Di Carlo, G.; Pantaleo, G.; Venezia, A.M.; Deganello, G.; Retailleau, L.; Boreave, A.; Giroir-Fendler, A. Supported Au catalysts for low-temperature abatement of propene and toluene, as model VOCs: Support effect. *Appl. Catal. B Environ.* **2011**, *101*, 629–637. [CrossRef]

122. Sun, Y.; Zhang, X.; Li, N.; Xing, X.; Yang, H.; Zhang, F.; Cheng, J.; Zhang, J.; Hao, Z. Surface properties enhanced Mn_xAlO oxide catalysts derived from Mn_xAl layered double hydroxides for acetone catalytic oxidation at low temperature. *Appl. Catal. B Environ.* **2019**, *251*, 295–304. [CrossRef]

123. Miao, L.; Tang, X.; Zhao, S.; Xie, X.; Du, C.; Tang, T.; Yi, H. Study on mechanism of low-temperature oxidation of n-hexanal catalysed by 2D ultrathin Co_3O_4 nanosheets. *Nano Res.* **2022**, *15*, 1660–1671. [CrossRef]

124. Mitsui, T.; Tsutsui, K.; Matsui, T.; Kikuchi, R.; Eguchi, K. Catalytic abatement of acetaldehyde over oxide-supported precious metal catalysts. *Appl. Catal. B Environ.* **2008**, *78*, 158–165. [CrossRef]

125. Zhu, X.; Zhang, S.; Yu, X.; Zhu, X.; Zheng, C.; Gao, X.; Luo, Z.; Cen, K. Controllable synthesis of hierarchical MnO_x/TiO_2 composite nanofibers for complete oxidation of low-concentration acetone. *J. Hazard. Mater.* **2017**, *337*, 105–114. [CrossRef] [PubMed]

126. Kim, S.C. The catalytic oxidation of aromatic hydrocarbons over supported metal oxide. *J. Hazard. Mater.* **2002**, *91*, 285–299. [CrossRef] [PubMed]

127. Lindhorst, A.C.; Schütz, J.; Netscher, T.; Bonrath, W.; Kühn, F.E. Catalytic oxidation of aromatic hydrocarbons by a molecular iron–NHC complex. *Catal. Sci. Technol.* **2017**, *7*, 1902–1911. [CrossRef]

128. Zhang, H.; Sui, S.; Zheng, X.; Cao, R.; Zhang, P. One-pot synthesis of atomically dispersed Pt on MnO_2 for efficient catalytic decomposition of toluene at low temperatures. *Appl. Catal. B Environ.* **2019**, *257*, 117878. [CrossRef]

129. Aghbolaghy, M.; Soltan, J.; Chen, N. Low temperature catalytic oxidation of binary mixture of toluene and acetone in the presence of ozone. *Catal. Lett.* **2018**, *148*, 3431–3444. [CrossRef]

130. Beauchet, R.; Mijoin, J.; Batonneau-Gener, I.; Magnoux, P. Catalytic oxidation of VOCs on NaX zeolite: Mixture effect with isopropanol and o-xylene. *Appl. Catal. B Environ.* **2010**, *100*, 91–96. [CrossRef]

131. Zhao, H.; Wang, H.; Qu, Z. Synergistic effects in Mn-Co mixed oxide supported on cordierite honeycomb for catalytic deep oxidation of VOCs. *J. Environ. Sci.* **2022**, *112*, 231–243. [CrossRef]

132. Zhao, H. *Preparation of Cobalt-Manganese and Cobalt-Copper Composite Oxides Monolithic Catalysts and Their Performance for VOCs Catalytic Oxidation*; Dalian University of Technology: Dalian, China, 2021.

133. Beauchet, R.; Magnoux, P.; Mijoin, J. Catalytic oxidation of volatile organic compounds (VOCs) mixture (isopropanol/o-xylene) on zeolite catalysts. *Catal. Today* **2007**, *124*, 118–123. [CrossRef]

134. Chu, S.; Wang, E.; Feng, F.; Zhang, C.; Jiang, J.; Zhang, Q.; Wang, F.; Bing, L.; Wang, G.; Han, D. A Review of Noble Metal Catalysts for Catalytic Removal of VOCs. *Catalysts* **2022**, *12*, 1543. [CrossRef]

135. Zhu, A.; Zhou, Y.; Wang, Y.; Zhu, Q.; Liu, H.; Zhang, Z.; Lu, H. Catalytic combustion of VOCs on Pt/CuMnCe and Pt/CeY honeycomb monolithic catalysts. *J. Rare Earths* **2018**, *36*, 1272–1277. [CrossRef]

136. Papaefthimiou, P.; Ioannides, T.; Verykios, X.E. Combustion of non-halogenated volatile organic compounds over group VIII metal catalysts. *Appl. Catal. B Environ.* **1997**, *13*, 175–184. [CrossRef]

137. Scire, S.; Minico, S.; Crisafulli, C.; Satriano, C.; Pistone, A. Catalytic combustion of volatile organic compounds on gold/cerium oxide catalysts. *Appl. Catal. B Environ.* **2003**, *40*, 43–49. [CrossRef]

138. Carabineiro, S.A.C.; Chen, X.; Martynyuk, O.; Bogdanchikova, N.; Avalos-Borja, M.; Pestryakov, A.; Tavares, P.B.; Órfão, J.J.M.; Figueiredo, J.L. Gold supported on metal oxides for volatile organic compounds total oxidation. *Catal. Today* **2015**, *244*, 103–114. [CrossRef]

139. Wang, J.; Zhong, J.; Gong, M.; Liu, Z.; Zhao, M.; Chen, Y. Remove cooking fume using catalytic combustion over $Pt/La-Al_2O_3$. *J. Environ. Sci.* **2007**, *19*, 644–646. [CrossRef] [PubMed]

140. Jianli, W.; Chuanwen, L.; Yongdong, C.; Hongyang, C.; Zhimin, L.; Maochu, G.; Yaoqiang, C. Low-temperature catalytic combustion of cooking fume over $Pt/\gamma-Al_2O_3/Ce_{0.5-x}Zr_{0.5-x}Mn_{2x}O_2$ monolithic catalyst. *Chin. J. Catal.* **2010**, *31*, 404–408.

141. Wang, J.; Zhong, J.; Gong, M.; Liu, Z.; Zhao, M.; Chen, Y. Removal of cooking fume by catalytic combustion on $Pt/La-Al_2O_3+Ce_{0.5}Zr_{0.5}O_2$ catalyst. *J. Rare Earths* **2006**, *24*, 633–635. [CrossRef]

142. Ho, Y.A.; Wang, S.Y.; Chiang, W.H.; Nguyen, V.H.; Chiu, J.L.; Wu, J.C.S. Moderate-temperature catalytic incineration of cooking oil fumes using hydrophobic honeycomb supported Pt/CNT catalyst. *J. Hazard. Mater.* **2019**, *379*, 120750. [CrossRef]

143. Sedjame, H.J.; Fontaine, C.; Lafaye, G.; Barbier, J., Jr. On the promoting effect of the addition of ceria to platinum based alumina catalysts for VOCs oxidation. *Appl. Catal. B Environ.* **2014**, *144*, 233–242. [CrossRef]

144. Barakat, T.; Idakiev, V.; Cousin, R.; Shao, G.S.; Yuan, Z.Y.; Tabakova, T.; Siffert, S. Total oxidation of toluene over noble metal based Ce, Fe and Ni doped titanium oxides. *Appl. Catal. B Environ.* **2014**, *146*, 138–146. [CrossRef]

145. Huang, S.; Zhang, C.; He, H. Complete oxidation of o-xylene over Pd/Al_2O_3 catalyst at low temperature. *Catal. Today* **2008**, *139*, 15–23. [CrossRef]

146. Liu, Y.; Deng, J.; Xie, S.; Wang, Z.; Dai, H. Catalytic removal of volatile organic compounds using ordered porous transition metal oxide and supported noble metal catalysts. *Chin. J. Catal.* **2016**, *37*, 1193–1205. [CrossRef]

147. Zhou, G.; He, X.; Liu, S.; Xie, H.; Fu, M. Phenyl VOCs catalytic combustion on supported CoMn/AC oxide catalyst. *J. Ind. Eng. Chem.* **2015**, *21*, 932–941. [CrossRef]

148. Yang, P.; Yang, S.; Shi, Z.; Meng, Z.; Zhou, R. Deep oxidation of chlorinated VOCs over CeO_2-based transition metal mixed oxide catalysts. *Appl. Catal. B Environ.* **2015**, *162*, 227–235. [CrossRef]

149. Chen, X.; Carabineiro, S.A.C.; Bastos, S.S.T.; Tavares, P.B.; Órfão, J.J.M.; Pereira, M.F.R.; Figueiredo, J.L. Exotemplated copper, cobalt, iron, lanthanum and nickel oxides for catalytic oxidation of ethyl acetate. *J. Environ. Chem. Eng.* **2013**, *1*, 795–804. [CrossRef]

150. Lin, L.Y.; Wang, C.Y.; Bai, H. A comparative investigation on the low-temperature catalytic oxidation of acetone over porous aluminosilicate-supported cerium oxides. *Chem. Eng. J.* **2015**, *264*, 835–844. [CrossRef]

151. Huang, Y.; Yi, H.; Tang, X.; Zhao, S.; Gao, F.; Wang, J.; Yang, Z. Cordierite-supported metal oxide for non-methane hydrocarbon oxidation in cooking oil fumes. *Environ. Technol.* **2018**. [CrossRef] [PubMed]

152. Pan, K.L.; Pan, G.T.; Chong, S.; Chang, M.B. Removal of VOCs from gas streams with double perovskite-type catalysts. *J. Environ. Sci.* **2018**, *69*, 205–216. [CrossRef]

153. Hosseini, S.A.; Salari, D.; Niaei, A.; Oskoui, S.A. Physical–chemical property and activity evaluation of $LaB_{0.5}Co_{0.5}O_3$ (B = Cr, Mn, Cu) and $LaMnxCo_{1-x}O_3$ (x = 0.1, 0.25, 0.5) nano perovskites in VOC combustion. *J. Ind. Eng. Chem.* **2013**, *19*, 1903–1909. [CrossRef]

154. Zhang, C.; Guo, Y.; Guo, Y.; Lu, G.; Boreave, A.; Retailleau, L.; Baylet, A.; Giroir-Fendler, A. LaMnO3 perovskite oxides prepared by different methods for catalytic oxidation of toluene. *Appl. Catal. B Environ.* **2014**, *148*, 490–498. [CrossRef]

155. Qin, Y.; Shen, F.; Zhu, T.; Hong, W.; Liu, X. Catalytic oxidation of ethyl acetate over $LaBO_3$ (B = Co, Mn, Ni, Fe) perovskites supported silver catalysts. *RSC Adv.* **2018**, *8*, 33425–33431. [CrossRef] [PubMed]

156. Arai, H.; Yamada, T.; Eguchi, K.; Seiyama, T. Catalytic combustion of methane over various perovskite-type oxides. *Appl. Catal.* **1986**, *26*, 265–276. [CrossRef]

157. Blasin-Aubé, V.; Belkouch, J.; Monceaux, L. General study of catalytic oxidation of various VOCs over $La_{0.8}Sr_{0.2}MnO_{3+x}$ perovskite catalyst—Influence of mixture. *Appl. Catal. B Environ.* **2003**, *43*, 175–186. [CrossRef]

158. Álvarez-Galván, M.C.; de La Peña O'Shea, V.A.; Arzamendi, G.; Pawelec, B.; Gandía, L.M.; Fierro JL, G. Methyl ethyl ketone combustion over La-transition metal (Cr, Co, Ni, Mn) perovskites. *Appl. Catal. B Environ.* **2009**, *92*, 445–453. [CrossRef]

159. Forni, L.; Rossetti, I. Catalytic combustion of hydrocarbons over perovskites. *Appl. Catal. B Environ.* **2002**, *38*, 29–37. [CrossRef]

160. Gu, W.; Li, C.; Qiu, J.; Yao, J. Facile preparation of porous hollow $CoxMn_{3-x}O_4$ normal-reverse coexisted spinel for toluene oxidation. *J. Alloy. Compd.* **2022**, *892*, 162185. [CrossRef]

161. Zhang, C.; Wang, J.; Yang, S.; Liang, H.; Men, Y. Boosting total oxidation of acetone over spinel MCo_2O_4 (M = Co, Ni, Cu) hollow mesoporous spheres by cation-substituting effect. *J. Colloid Interface Sci.* **2019**, *539*, 65–75. [CrossRef]

162. Zhang, Y.; Zeng, Z.; Li, Y.; Hou, Y.; Hu, J.; Huang, Z. Effect of the A-site cation over spinel AMn_2O_4 (A = Cu^{2+}, Ni^{2+}, Zn^{2+}) for toluene combustion: Enhancement of the synergy and the oxygen activation ability. *Fuel* **2021**, *288*, 119700. [CrossRef]

163. Zhang, S.; Liu, S.; Zhu, X.; Yang, Y.; Hu, W.; Zhao, H.; Qu, R.; Zheng, C.; Gao, X. Low temperature catalytic oxidation of propane over cobalt-cerium spinel oxides catalysts. *Appl. Surf. Sci.* **2019**, *479*, 1132–1140. [CrossRef]

164. Kim, D.C.; Ihm, S.K. Application of spinel-type cobalt chromite as a novel catalyst for combustion of chlorinated organic pollutants. *Environ. Sci. Technol.* **2001**, *35*, 222–226. [CrossRef]

165. Rezlescu, N.; Rezlescu, E.; Popa, P.D.; Popovici, E.; Doroftei, C.; Ignat, M. Preparation and characterization of spinel-type $MeFe_2O_4$ (Me = Cu, Cd, Ni and Zn) for catalyst applications. *Mater. Chem. Phys.* **2013**, *137*, 922–927. [CrossRef]

166. Zavyalova, U.; Nigrovski, B.; Pollok, K.; Langenhorst, F.; Müller, B.; Scholz, P.; Ondruschka, B. Gel-combustion synthesis of nanocrystalline spinel catalysts for VOCs elimination. *Appl. Catal. B Environ.* **2008**, *83*, 221–228. [CrossRef]

167. Yang, B.L.; Chan, S.F.; Chang, W.S.; Chen, Y.Z. Surface enrichment in mixed oxides of Cu, Co, and Mn, and its effect on CO oxidation. *J. Catal.* **1991**, *130*, 52–61. [CrossRef]

168. Maltha, A.; Kist, H.F.; Brunet, B.; Ziolkowski, J.; Onishi, H.; Iwasawa, Y.; Ponec, V. The active sites of manganese-and cobalt-containing catalysts in the selective gas phase reduction of nitrobenzene. *J. Catal.* **1994**, *149*, 356–363. [CrossRef]

169. Li, Y.; Zhang, T.T.; Wang, J.; Zhu, Z.; Jia, B.; Yu, J. Catalytic Combustion of n-Hexanal Using Cu-Mn Composite Oxide Supported on TiO_2. *Acta Phys. -Chim. Sin.* **2016**, *32*, 2084–2092. [CrossRef]

170. Behar, S.; Gonzalez, P.; Agulhon, P.; Quignard, F.; Świerczyński, D. New synthesis of nanosized Cu–Mn spinels as efficient oxidation catalysts. *Catal. Today* **2012**, *189*, 35–41. [CrossRef]

171. Yi, H.; Huang, Y.; Tang, X.; Zhao, S.; Gao, F.; Wang, J.; Yang, Z. Mn-CeO_x/MeO_x (Ti, Al)/cordierite preparation with ultrasound-assisted for non-methane hydrocarbon removal from cooking oil fumes. *Ultrason. Sonochemistry* **2019**, *53*, 126–133. [CrossRef]

172. Xu, S.Y.; Li, S.; Peng, D.H.; Zhang, X.H.; Ge, W.L.; Qian, J.Z. Catalytic Degradation of n-Heptane over Cu/Co Composite Oxides. *Fine Chem.* **2018**, *35*, 402–409.